Immunogenetics (2013) 65:107–114
DOI 10.1007/s00251-012-0663-8

ORIGINAL PAPER

MxA transcripts with distinct first exons and modulation of gene expression levels by single-nucleotide polymorphisms in human bronchial epithelial cells

Satoshi Noguchi · Minako Hijikata · Emi Hamano · Ikumi Matsushita · Hideyuki Ito · Jun Ohashi · Takahide Nagase · Naoto Keicho

Received: 3 September 2012 / Accepted: 22 October 2012 / Published online: 18 November 2012

Abstract Myxovirus resistance A (MxA) is a major interferon (IFN)-inducible antiviral protein. Promoter single-nucleotide polymorphisms (SNPs) of MxA near the IFN-stimulated response element (ISRE) have been frequently associated with various viral diseases, including emerging respiratory infections. We investigated the expression profile of MxA transcripts with distinct first exons in human bronchial epithelial cells. For primary culture, the bronchial epithelium was isolated from lung tissues with different genotypes, and total RNA was subjected to real-time reverse transcription polymerase chain reaction. The previously reported MxA transcript (T1) and a recently registered transcript with a distinct 5′ first exon (T0) were identified. IFN-β and polyinosinic–polycytidylic acid induced approximately 100-fold higher expression of the T1 transcript than that of the T0 transcript, which also had a potential ISRE motif near its transcription start site. Even without inducers, the T1 transcript accounted for approximately two thirds of the total expression of MxA, levels of which were significantly associated with its promoter and exon 1 SNPs (rs17000900, rs2071430, and rs464138). Our results suggest that MxA observed in respiratory viral infections is possibly dominated by the T1 transcript and partly influenced by relevant 5′ SNPs.

Keywords Myxovirus resistance A · Single-nucleotide polymorphism · Human bronchial epithelial cells · Transcript variants

Abbreviations

LD	Linkage disequilibrium
HBE	Human bronchial epithelial
ISRE	Interferon-stimulated response element

Introduction

The interferon (IFN) system plays an important role in innate immunity against pathogens. When viral components are detected by pattern recognition receptors, infected cells produce type I (α and β) and type III (λ) IFNs (Randall and Goodbourn 2008). Binding of IFNs to their specific receptors leads to the induction of more than 300 IFN-stimulated genes, including myxovirus resistance A (MxA), also known as the myxovirus (influenza virus) resistance 1, IFN-inducible protein p78 (mouse) (MX1) gene. Following

Electronic supplementary material The online version of this article (doi:10.1007/s00251-012-0663-8) contains supplementary material, which is available to authorized users.

S. Noguchi · M. Hijikata · E. Hamano · I. Matsushita · N. Keicho (✉)
Department of Respiratory Diseases, Research Institute, National Center for Global Health and Medicine, 1-21-1 Toyama, Shinjuku-ku, Tokyo 162-8655, Japan
e-mail: nkeicho-tky@umin.ac.jp

S. Noguchi · E. Hamano · T. Nagase
Department of Respiratory Medicine, University of Tokyo Hospital, Tokyo 113-0033, Japan

H. Ito
Department of Thoracic Surgery, National Center for Global Health and Medicine, Tokyo 162-8655, Japan

J. Ohashi
Molecular and Genetic Epidemiology, Faculty of Medicine, University of Tsukuba, Ibaraki 305-8575, Japan

IFN-induced expression, MxA is thought to form oligomeric rings around the nucleocapsid structures of viruses, thereby inhibiting their transcriptional and replicative functions (Haller and Kochs 2011).

The promoter of the human MxA transcript in the original report contains two IFN-stimulated response elements (ISRE), ISRE1 and ISRE2, near the transcription start site, and both are involved in IFN responsiveness (Ronni et al. 1998). The IFN-stimulated gene factor 3 complex binds to the most proximal ISRE1 and the second ISRE2. ISRE1 is essential for MxA promoter activation, whereas ISRE2 has an enhancing effect in the presence of activated ISRE1 (Ronni et al. 1998). IFN regulatory factor 3 can only bind to ISRE2 for enhancing promoter activation (Holzinger et al. 2007). Around ISRE2, there are two single-nucleotide polymorphisms (SNPs) at nucleotide positions −88 and −123, which confer differences in the promoter activity and binding affinity to nuclear proteins (Hijikata et al. 2001; Ching et al. 2010). Promoter SNPs of MxA are reportedly associated with diseases, including hepatitis C (Hijikata et al. 2000; Hijikata et al. 2001), hepatitis B (Peng et al. 2007), multiple sclerosis (Furuyama et al. 2006), and subacute sclerosing panencephalitis (Torisu et al. 2004). We previously reported the association of MxA promoter SNP with the severity of severe acute respiratory syndrome (SARS; Hamano et al. 2005), and Ching et al. (2010) reported its association with susceptibility to SARS in a larger case–control study. However, the expression levels of MxA have been analyzed only in peripheral blood mononuclear cells (PBMC) or liver cells (Fernandez-Arcas et al. 2004; Kong et al. 2007; Abe et al. 2011; McGilvray et al. 2012).

Because MxA has a pivotal role in host defense against not only SARS coronavirus but also other respiratory viruses such as influenza virus (Haller and Kochs 2011), it is important to characterize the expression profile of MxA in human bronchial epithelial (HBE) cells, a site for replication of many respiratory viruses. In addition, a new transcript variant with alternative 5′ untranslated exons starting 5.5 kb upstream of the original exon 1 has recently been registered in the public database (NM_001144925.1). In the present study, we analyzed the expression patterns of MxA transcripts with distinct first exons. We further investigated the possible effects of their 5′ SNPs on gene expression levels in a panel of primary cultured HBE cells with different genotypes.

Materials and methods

Cell culture

The study protocol was approved by the ethical committee of the National Center for Global Health and Medicine (formerly, International Medical Center of Japan). Primary cultured HBE cells were obtained from the cancer-free bronchi of surgically resected lungs after obtaining written informed consent from the individuals concerned, all of whom were Japanese. HBE cells (n=38) were isolated and cultured as described previously (Gray et al. 1996) and used after three–five passages in this study. In brief, HBE cells were seeded at a density of 5×10^5/well onto collagen-coated six-well Transwell plates (Corning Inc., Corning, NY, USA) and cultured in bronchial epithelial growth medium (Bio-Whittaker, Walkersville, MD, USA) for 24 h. Thereafter, HBE cells (n=3) were stimulated with 1,000 IU/ml IFN-α (PeproTech EC Ltd., London W6 8LL, UK), 1,000 IU/ml IFN-β (Biosource International, Camarillo, CA, USA), 100 μg/ml polyinosinic–polycytidylic acid [poly(I:C); Sigma-Aldrich, St. Louis, MO, USA], 10 ng/ml IFN-γ (R&D Systems, Minneapolis, MN, USA), 50 ng/ml TNF-α (R&D Systems), 20 μg/ml lipopolysaccharide (LPS; Sigma-Aldrich), 10 μg/ml α-defensin 1 (Peptide Institute Inc., Osaka, Japan), 10 μg/ml β-defensin 1 (Peptide Institute Inc.), and 10 μg/ml β-defensin 2 (Peptide Institute Inc.) for 24 h and then harvested. Unstimulated HBE cells (n=38) and those stimulated with 100 μg/ml poly(I:C) for 24 h (n=29) or with 1,000 IU/ml IFN-β for 12 h (n=9) were harvested, and gene expression levels were then analyzed. To assess time-dependent changes in mRNA expression, BEAS-2B cells (ATCC number CRL-9609) were stimulated with 100 μg/ml poly(I:C) for 6, 12, 24, and 48 h.

Real-time reverse transcription polymerase chain reaction

We designated the MxA transcript originally reported by Horisberger et al. (1990) (NM_002462.3) as the T1 transcript and the new transcript variant in the public database (NM_001144925.1) as the T0 transcript. Distinct exons used in the T0 transcript are shown as exons 0a, 0b, and 0c (Fig. 1). Translational start codons of both the T1 and T0 transcripts originate from exon 5, indicating that exons 0a–0c and exons 1–4 are all 5′ untranslated exons.

Total RNA of the cells was extracted using the RNeasy Mini Kit (Qiagen, Hamburg, Germany). Human Total RNA Master panel II (Clontech, Mountain View, CA, USA) was used to investigate gene expression in various tissue types. Most of the tissue RNA in this panel consisted of pooled RNA from two or more donors, and their genotypes were not available. One microgram of total RNA was subjected to RT with random nonamers using SuperScript III Reverse Transcriptase (Invitrogen, Carlsbad, CA, USA). MxA mRNA expression was analyzed by real-time reverse transcription polymerase chain reaction (RT-PCR) using SYBR Premix Ex Taq (Takara Bio, Shiga, Japan) and CFX96 (BioRad, Hercules, CA, USA). Sense and antisense primers were located in exons 0b and 0c (5′-CCAGAGCAACTCCACACCGGGTGC-3′ and 5′-GCTATGGTTCCAATCCAGGTGATC-3′) for the T0 transcript and exons 1 and 2

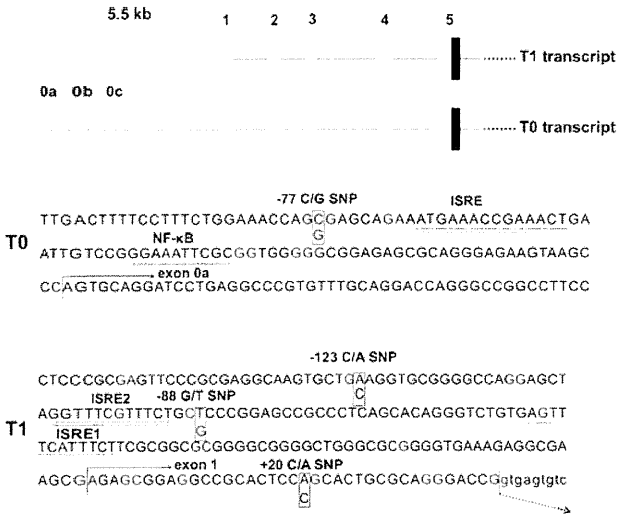

Fig. 1 Alternate splicing of 5′ exons in MxA. The 5′ genomic structure of MxA and nucleotide sequences around the transcription start sites of the T0 and T1 transcripts are shown. *White boxes* represent the untranslated mRNA sequence, and *black boxes* represent the translated sequence. Potential ISREs are *double underlined*, NF-κB binding site is *underlined*, and promoter and exon 1 SNPs are *boxed*. The transcription start site (Horisberger et al. 1990) and nucleotide positions shown in the T1 transcript are displayed in accordance with MxA promoter analysis by Ronni et al. (1998)

(5′-GCACTGCGCAGGGACCG-3′ and 5′-TGGG-TGAG-CAGGTGGGCGGCA-3′) for the T1 transcript. PCR conditions consisted of 40 cycles of denaturation for 15 s at 95 °C and annealing and extension for 1 min at 60 °C. Specific target amplification was confirmed by a single peak in the dissociation curve. The mRNA copy numbers between different transcripts were compared using the absolute quantification method (Leong et al. 2007). RT-PCR products were purified using the Wizard PCR Preps DNA Purification System (Promega, Fitchburg, WI, USA), and their copy numbers were calculated from the DNA concentration determined by measuring the absorbance at 260 nm. The standard curve was generated with a serial fivefold dilution of each RT-PCR product, and the linear dependence of the threshold cycles was confirmed from the template concentrations. We used the β-actin gene (primers listed in Online Resource 1) to normalize the expression of MxA for calculating the relative amounts of mRNA of each transcript. The TaqMan Gene Expression Assay (Hs00182073_m1) (Applied Biosystems, Foster City, CA, USA) that amplifies exons 16–17 of MxA was used with TaqMan Universal Master Mix II (Applied Biosystems) in the StepOne Plus Real-Time PCR System (Applied Biosystems), and the relative amount of total transcripts, indicating the overall expression of MxA, was calculated using the standard curve method with glyceraldehyde 3-phosphate dehydrogenase as an internal control.

Rapid amplification of 5′ cDNA end

RNA ligase-mediated rapid amplification of 5′ cDNA end (5′ RACE) was performed using total RNA from IFN-β-stimulated HBE cells to determine the transcription start site of T0 using the First-Choice RLM-RACE Kit (Ambion, Austin, TX, USA). Gene-specific primers are listed in Online Resource 1. PCR products were sequenced with the BigDye Terminator v3.1 Cycle Sequencing Kit (Applied Biosystems) using a 3130xl Genetic Analyzer (Applied Biosystems).

Screening and genotyping of polymorphisms in the 5′ region

Genomic DNA was extracted from HBE cells (n=38) using the QIAamp DNA Mini Kit (Qiagen). The 5′ upstream region of the transcription start site for the T0 transcript was amplified with two overlapping PCR products, and the amplified products were sequenced using appropriate inner primers. Three SNPs, −123 C/A (rs17000900), −88 G/T (rs2071430), and +20 C/A (rs464138), two in the promoter and one in exon 1 of the T1 transcript, were genotyped by PCR and restriction fragment length polymorphism methods (Hamano et al. 2005), with Pst I (Takara Bio) for rs17000900, Hha I (Takara Bio) for rs2071430, and Bpm I (New England Biolabs, Ipswich, MA, USA) for rs464138. The primers are listed in Online Resource 1. Linkage disequilibrium (LD) between promoter SNPs was analyzed using Haploview (v. 4.2) (Barrett et al. 2005).

Statistical analysis

All data were expressed as mean±standard error of the mean (SEM). To assess the relationship between the number of single alleles of −123 C/A, −88 G/T, and +20 C/A SNPs and expression levels of the transcript variants, a simple linear regression model was applied (JMP, version 9.0.0; SAS Institute Inc., Cary, NC, USA). A multiple linear regression model was also applied to assess the combined effects of these SNPs on expression of the T1 transcript. The numbers of alleles of the three abovementioned SNPs were incorporated in the model as explanatory variables. Correlations of the total amount of the MxA transcripts with expression levels of the T0 and T1 transcripts were further analyzed using Spearman's rank correlation coefficient. A p value <0.05 was considered to be statistically significant.

Results

Expression patterns of MxA transcripts in human tissues

The originally reported MxA transcript, T1, and a recently registered transcript variant, T0, were both successfully

amplified by RT-PCR from various human tissues (Fig. 2). Expression of the T1 transcript was predominant in the tissues examined, including the lung and trachea, whereas expression of the T0 transcript was inconspicuous, except in the testis and adrenal gland.

Induction patterns of MxA transcripts in HBE cells incubated with type I IFNs and other stimuli

MxA transcripts, T0 and T1, were both detected in the unstimulated primary cultured HBE cells (n=3), and their expression was markedly induced by type I IFNs and poly(I:C), although induction of the T1 transcript was much stronger than that of the T0 transcript (Fig. 3). IFN-γ, TNF-α, and α-defensin 1 also induced expression of the T1 transcript to a lesser extent, whereas this increase was not observed in the T0 transcript.

Genomic structure and genetic polymorphisms in the 5′ upstream regions of MxA transcripts with distinct first exons

Because the transcript variant T0 with alternatively spliced exons was moderately induced by type I IFNs, 5′ RACE was performed to determine the 5′ end of exon 0a, the transcription start site of T0, in IFN-β-stimulated HBE cells (Fig. 1). A putative ISRE motif and a possible binding site for NF-κB were revealed in the 5′ upstream region of the T0 transcript (Fig. 1). The nearly full-length transcript T0 was amplified with the sense primer in exon 0c and the antisense primer in the last exon 17; however, no alternatively spliced exon was observed in the protein-coding region (data not shown). Although the transcript variant that skips untranslated exons 2

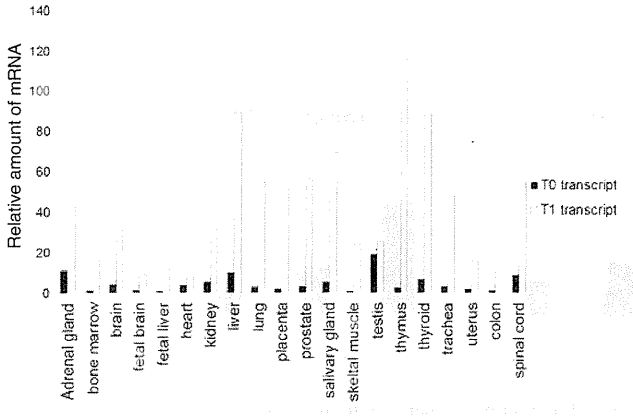

Fig. 2 Relative expression levels of two MxA transcript variants in human tissues. Relative expression levels of the T0 and T1 transcripts in various human tissues were obtained by real-time RT-PCR using a commercial RNA panel, Human Total RNA Master panel II (Clontech). The RNA consisted of pooled RNA from two or more donors. Their genotypes were not available but presumably mixture of different genotypes

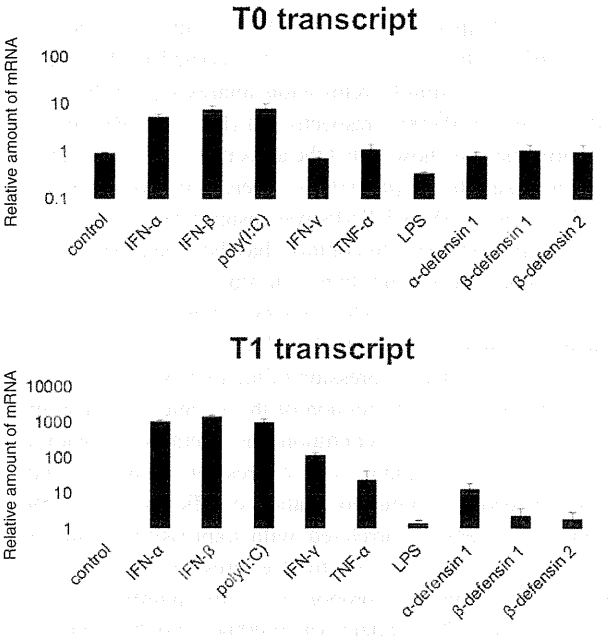

Fig. 3 Induction of T0 and T1 transcript variants by various stimuli in HBE cells. HBE cells (n=3) were stimulated with IFN-α, IFN-β, poly (I:C), IFN-γ, TNF-α, LPS, α-defensin 1, β-defensin 1, and β-defensin 2 for 24 h and then harvested. Expression levels of the T0 and T1 transcripts were compared with those of unstimulated cells by real-time RT-PCR. Fold inductions are shown as the mean±SEM. The genotypes of the promoter SNPs were as follows: sample #1, −77 SNP (rs457274) C/G, −123 SNP (rs17000900) C/A, −88 SNP (rs2071430) G/T, and +20 SNP (rs464138) C/A; sample #2, −77 C/C, −123 C/A, −88 T/T, and +20 A/A and; sample #3, −77 C/G, −123 C/C, −88 G/G, and +20 C/A

and 4 has also been registered in the public database (NM_001178046.1), its expression level was very low in the HBE cells (data not shown).

Sequence analysis of the 5′ upstream region of the T0 transcript using our DNA samples identified genomic variations, −77 C/G SNP (rs457274) near the putative ISRE motif (Fig. 1), −326 deletion/insertion polymorphism (rs60467231), and −504 A/G SNP (rs12483338). Three other SNPs, −123 C/A (rs17000900), −88 G/T (rs2071430), and +20 C/A (rs464138), near the 5′ end of the T1 transcript were also detected (Fig. 1). As shown in Online Resource 2, −77 C/G SNP of the T0 transcript and the three SNPs near the 5′ end of the T1 transcript were all in strong LD with each other (D'> 0.8, r^2>0.4).

Differences in expression levels of MxA among SNP genotypes

Next, the mRNA expression levels of the T0 and T1 transcripts were analyzed in HBE cells with different genotypes. The expression of the T1 transcript assessed by real-time RT-PCR was 2.3-fold higher than that of the T0 transcript under the unstimulated condition (n=38). Baseline expression of the T1 transcript was significantly higher in proportion to the

number of A alleles of −123 C/A SNP, T alleles of −88 G/T SNP, and A alleles of +20 C/A SNP carried by HBE cells according to a simple regression analysis (p=0.013, p=0.0035, and p<0.0001, respectively) (Fig. 4b). Multiple regression analysis showed that the association of +20 C/A SNP remained significant (p=0.016), whereas the association of −123 C/A and −88 G/T SNPs was insignificant (p=0.67 and p=0.78, respectively). In contrast, baseline expression of the T0 transcript was slightly higher in proportion to the number of C alleles of −77 C/G SNP; however, this increase was not statistically significant (p=0.086) (Fig. 4a).

When the relative expression of the total MxA transcripts was compared with expression of the T1 and T0 transcripts under the unstimulated condition, the overall expression of MxA strongly correlated with expression of the T1 transcript (Spearman's rank correlation coefficient; rs=0.759), whereas it weakly correlated with expression of the T0 transcript (rs=0.388). The total expression of MxA was significantly higher in proportion to the number of −123 A, −88 T, and +20 A alleles (p=0.0004, p<0.0001, and p<0.0001, respectively), which was similar to the linear relationship between the T1 transcript and number of alleles shown above.

When immortalized HBE cell line BEAS-2B was stimulated with poly(I:C), time-course analysis revealed that expression of the T0 transcript was the highest after 24 h, whereas that of the T1 transcript was the highest after 6–12 h of incubation (Online Resource 3). We therefore investigated the expression of T0 and T1 transcripts in HBE cells (n=29) stimulated with poly(I:C) for 24 h. The expression of the T0 transcript increased eightfold, whereas that of the T1 transcript increased 870-fold. Poly(I:C)-induced expression of both transcripts was not associated with either allele of the four SNPs (Fig. 5a, b). When HBE cells (n=9) were stimulated with IFN-β for 12 h, the T0 transcript was induced eightfold, and the T1 transcript was induced 640-fold. IFN-β-induced expression of the transcripts did not vary among genotypes (data not shown).

Discussion

In this study, we investigated the expression profile of MxA by analyzing expression of the original transcript T1 and the transcript variant T0 in primary cultured HBE cells. According to our absolute quantification method using real-time RT-PCR, the amount of the T0 transcript was approximately half of that of the T1 transcript at the baseline level. Although expression of the T0 transcript was also induced by type I IFNs and poly(I:C) and its 5′ proximal region has a potential ISRE motif, IFN-β and poly(I:C) inducibility of the T1 transcript was at least 100-fold higher than that of the

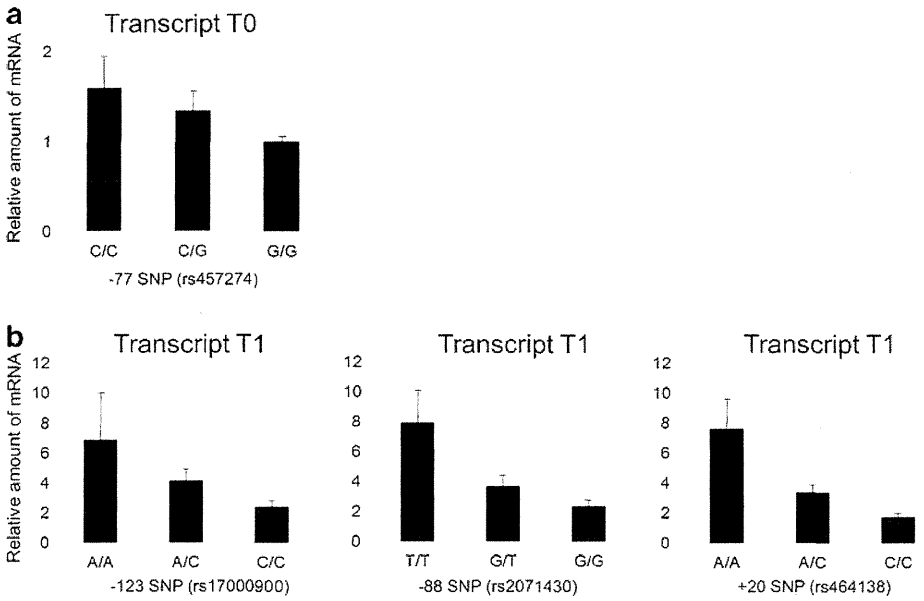

Fig. 4 Differences in the baseline expression of transcript variants among the genotypes of the promoter and exon 1 SNPs in HBE cells. Expression of **a** T0 and **b** T1 transcripts under the unstimulated condition in HBE cells with each genotype of −77 C/G SNP for the T0 transcript (C/C, n=8; C/G, n=18; G/G, n=12), of −123 C/A SNP (A/A, n=2; A/C, n=18; C/C, n=18), of −88 G/T SNP (T/T, n=3; G/T, n=19; G/G, n=16), and of +20 C/A SNP (A/A, n=5; A/C, n=22; C/C, n=11) for the T1 transcript is shown. The relative amounts of mRNA of each transcript compared with that of the T0 transcript in GG cells without poly(I:C) stimulation are shown as mean±SEM. Possible associations between the number of alleles and the amount of the corresponding transcripts were assessed by a simple regression model respectively (p=0.086 for the number of −77 C alleles, p=0.013 for −123 A alleles, p=0.0035 for −88 T alleles, and p<0.0001 for +20 A alleles)

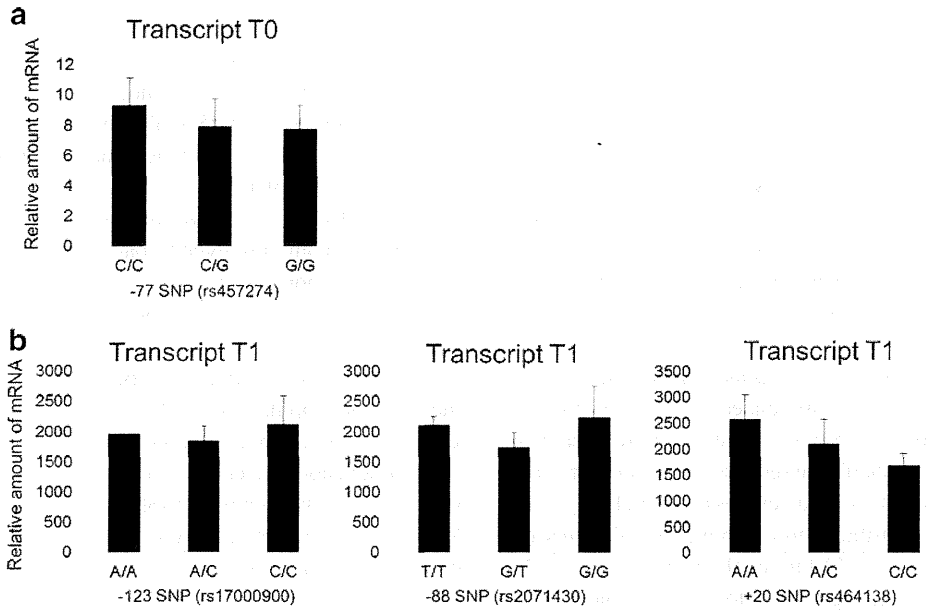

Fig. 5 Differences in the poly(I:C)-induced expression of transcript variants among the genotypes of the promoter and exon 1 SNPs in HBE cells. Expression of **a** T0 and **b** T1 transcripts in the presence of poly(I:C) in HBE cells with each genotype of −77 C/G SNP for the T0 transcript (C/C, n=5; C/G, n=13; G/G, n=11), of −123 C/A SNP (A/A, n=1; A/C, n=12; C/C, n=16), of −88 G/T SNP (T/T, n=2; G/T, n=13; G/G, n=14), and of +20 C/A SNP (A/A, n=3; A/C, n=16; C/C, n=10) for the T1 transcript is shown. The relative amounts of mRNA of each transcript compared with that of the T0 transcript in GG cells without poly(I:C) stimulation are shown as mean±SEM. Possible associations were assessed by a simple regression model (p=0.647 for the number of −77 C alleles, p=0.662 for −123 A alleles, p=0.539 for −88 T alleles, and p=0.331 for +20 A alleles)

T0 transcript. This observation implies that MxA response to viral infection of respiratory cells is mostly controlled by the expression of the T1 transcript.

Remarkably increased levels of the T1 transcript after stimulation with type I IFNs or an IFN-inducing agent, poly(I:C), were consistent with the general consensus that the induction of MxA requires type I or type III IFN signaling (Haller and Kochs 2011). However, levels of the T1 transcript were also elevated in HBE cells by other physiological stimuli. Moderate elevation of levels of the T1 transcript in the presence of IFN-γ and TNF-α may be mediated by the secondary induction of type I or type III IFNs. Although Mahanonda et al. (2012) demonstrated the induction of MxA by α-defensin in primary human gingival epithelial cells, the mechanism by which the T1 transcript was upregulated by α-defensin remains unknown. These observations support the idea that the T1 transcript plays a major role in airway diseases.

We also analyzed the expression of T0 transcript with alternative 5′ untranslated exons. Alternative promoter usage is now recognized as a common mechanism in the transcriptional regulation of mammalian genes (Davuluri et al. 2008). Among IFN-stimulated genes, ADAR1 was shown to have alternative promoters (George and Samuel 1999): one promoter contributes to constitutive expression and the other to inducible expression. To our knowledge, no IFN-stimulated genes other than MxA, whose antiviral function is well known (Sadler and Williams 2008), have been reported to possess two IFN-inducible transcripts with distinct first exons. The molecular mechanism for tissue specificity of these transcripts is unknown; however, of note, the promoter of the T0 transcript contains the putative steroidogenic factor-1 binding site (position −636 to −644) thought to be important to testis- and adrenal gland-specific gene expression (Schimmer and White 2010). A study of the expression profiles of MxA in various organs would be interesting.

Although IFN-mediated upregulation of the T0 transcript was moderate in contrast to that of the T1 transcript, baseline levels of the T0 transcript were not negligible in HBE cells. It is thus conceivable that the T0 transcript plays a minor but independent role in the human airway. Furthermore, considering the difference between the time course of mRNA expression of the T0 and T1 transcripts after poly(I:C) stimulation, it is likely that other factors further modulate their induction levels. Because some reports (Aebi et al. 1989; Goetschy et al. 1989; Prescott et al. 2005) indicate the presence of IFN-independent induction of MxA in contrast to the results of Holzinger et al. (2007), it would be worth investigating whether the T0 transcript can be induced through an IFN-independent signaling system in viral infection.

We observed the regulatory effects of −123, −88, and +20 SNPs on mRNA levels of the T1 transcript in HBE cells

under the unstimulated condition. When we evaluated the overall expression of the MxA transcripts by real-time RT-PCR, it was found to be closely correlated with levels of the T1 transcript, suggesting that individual variation of the total expression of MxA is mainly explained by the T1 transcript. Indeed overall levels of MxA as well as expression of the T1 transcript were strongly associated with these three SNPs at baseline levels. It has been repeatedly reported that the minor A allele of −123 SNP and the minor T allele of −88 SNP, which are in strong LD, were associated with the overall transcriptional activity of the gene (Hijikata et al. 2001; Torisu et al. 2004). Expression of MxA was associated with −88 G/T SNP when PBMC cells were stimulated with IFN-α2 for 12 h (Fernandez-Arcas et al. 2004). In one study (Furuyama et al. 2006), the results of a luciferase reporter assay suggested that −123 SNP contributed to basal expression levels of MxA, whereas −88 SNP contributed to the induction of expression by IFNs. Ching et al. (2010) further showed that the −123A allele had a stronger binding affinity to nuclear proteins from unstimulated cells and that the −88 T allele preferentially bound to the protein after IFN-β stimulation. In our study using HBE cells, −123, −88, and +20 SNPs were all associated with baseline expression of the T1 transcript, and according to a multiple regression analysis, among the three SNPs, +20 C/A SNP was still associated with baseline expression of the T1 transcript. This finding may be attributed to the difference in cell type; however, extensive investigation is required to determine the possible effect of +20 SNP or other unknown functional polymorphisms in strong LD. Recently, Tran Thi Duc et al. (2012) reported that three SNPs (−309 C/G, −101 G/A, and +20 C/A) also contributed to the promoter activity in combination with well-known effects of −123 and −88 SNPs. We could not examine −309 and −101 SNPs in our samples because −309 C/G and −101 G/A SNPs were detected only in the African population and their minor allele frequencies were relatively low (Duc et al. 2012).

Under the poly(I:C)-stimulated condition, the +20 SNP also tended to be associated with expression of the T1 transcript in our study; however, this tendency was not statistically significant. When HBE cells were stimulated with IFN-β for 12 h, the same three SNPs were not associated with the expression level. These findings may conflict with the in vitro effects of these 5′ SNPs on the IFN-inducible promoter activity previously assessed by a luciferase reporter system (Hijikata et al. 2001; Torisu et al. 2004; Tran Thi Duc et al. 2012). In our study, however, the mRNA induced by poly (I:C), the dsRNA analog to mimic viral infection, was directly assessed in primary cultured HBE cells, which implies that individual variance of relevant factors such as toll-like receptor 3 and subsequent IFN signaling pathways might have affected the mRNA levels in the IFN-stimulated condition and have masked the independent effects of these promoter SNPs of the MxA gene.

We previously reported that the promoter −88 SNP was associated with severity of SARS in the Vietnamese population (Hamano et al. 2005), and the promoter −123 SNP was associated with SARS in the Chinese population (Ching et al. 2010). According to Chen and Subbarao (2007), IFN induction is completely suppressed in SARS coronavirus-infected cells. Our ex vivo findings that these regulatory SNPs were mainly involved in baseline expression of the T1 transcript support the results of these disease association studies. However, we could not show significant difference in the regulatory effects between −88 and −123 SNPs, possibly because of strong LD between these two SNPs in the Japanese population (r^2=0.83) compared with moderate LD in the Chinese population (r^2=0.39) (Ching et al. 2010).

In conclusion, we characterized the expression profile of the previously known transcript and the transcript variant of MxA and demonstrated a significant effect of its 5′ SNPs on basal expression of the overall transcripts in HBE cells. Our findings may lead to an improved understanding of the association of MxA SNPs with susceptibility to respiratory viral infections.

Acknowledgments We thank Keiko Wakabayashi for technical assistance in the study. This work was partly supported by a grant from the National Center for Global Health and Medicine.

Conflict of interest All authors have no conflict of interest on this work.

References

Abe H, Hayes CN, Ochi H, Maekawa T, Tsuge M, Miki D, Mitsui F, Hiraga N, Imamura M, Takahashi S, Kubo M, Nakamura Y, Chayama K (2011) IL28 variation affects expression of interferon stimulated genes and peg-interferon and ribavirin therapy. J Hepatol 54:1094–1101

Aebi M, Fah J, Hurt N, Samuel CE, Thomis D, Bazzigher L, Pavlovic J, Haller O, Staeheli P (1989) cDNA structures and regulation of two interferon-induced human Mx proteins. Mol Cell Biol 9:5062–5072

Barrett JC, Fry B, Maller J, Daly MJ (2005) Haploview: analysis and visualization of LD and haplotype maps. Bioinformatics 21:263–265

Chen J, Subbarao K (2007) The immunobiology of SARS. Annu Rev Immunol 25:443–472

Ching JC, Chan KY, Lee EH, Xu MS, Ting CK, So TM, Sham PC, Leung GM, Peiris JS, Khoo US (2010) Significance of the myxovirus resistance A (MxA) gene −123C>a single-nucleotide polymorphism in suppressed interferon beta induction of severe acute respiratory syndrome coronavirus infection. J Infect Dis 201:1899–1908

Davuluri RV, Suzuki Y, Sugano S, Plass C, Huang TH (2008) The functional consequences of alternative promoter use in mammalian genomes. Trends Genet 24:167–177

Duc TT, Farnir F, Michaux C, Desmecht D, Cornet A (2012) Detection of new biallelic polymorphisms in the human MxA gene. Mol Biol Rep 39:8533–8538

Fernandez-Arcas N, Blanco A, Gaitan MJ, Nyqvist M, Alonso A, Reyes-Engel A (2004) Differential transcriptional expresion of

the polymorphic myxovirus resistance protein A in response to interferon-alpha treatment. Pharmacogenetics 14:189–193

Furuyama H, Chiba S, Okabayashi T, Yokota S, Nonaka M, Imai T, Fujii N, Matsumoto H (2006) Single nucleotide polymorphisms and functional analysis of MxA promoter region in multiple sclerosis. J Neurol Sci 249:153–157

George CX, Samuel CE (1999) Human RNA-specific adenosine deaminase ADAR1 transcripts possess alternative exon 1 structures that initiate from different promoters, one constitutively active and the other interferon inducible. Proc Natl Acad Sci U S A 96:4621–4626

Goetschy JF, Zeller H, Content J, Horisberger MA (1989) Regulation of the interferon-inducible IFI-78K gene, the human equivalent of the murine Mx gene, by interferons, double-stranded RNA, certain cytokines, and viruses. J Virol 63:2616–2622

Gray TE, Guzman K, Davis CW, Abdullah LH, Nettesheim P (1996) Mucociliary differentiation of serially passaged normal human tracheobronchial epithelial cells. Am J Respir Cell Mol Biol 14:104–112

Haller O, Kochs G (2011) Human MxA protein: an interferon-induced dynamin-like GTPase with broad antiviral activity. J Interferon Cytokine Res 31:79–87

Hamano E, Hijikata M, Itoyama S, Quy T, Phi NC, Long HT, Ha LD, Ban VV, Matsushita I, Yanai H, Kirikae F, Kirikae T, Kuratsuji T, Sasazuki T, Keicho N (2005) Polymorphisms of interferon-inducible genes OAS-1 and MxA associated with SARS in the Vietnamese population. Biochem Biophys Res Commun 329:1234–1239

Hijikata M, Mishiro S, Miyamoto C, Furuichi Y, Hashimoto M, Ohta Y (2001) Genetic polymorphism of the MxA gene promoter and interferon responsiveness of hepatitis C patients: revisited by analyzing two SNP sites (−123 and −88) in vivo and in vitro. Intervirology 44:379–382

Hijikata M, Ohta Y, Mishiro S (2000) Identification of a single nucleotide polymorphism in the MxA gene promoter (G/T at nt −88) correlated with the response of hepatitis C patients to interferon. Intervirology 43:124–127

Holzinger D, Jorns C, Stertz S, Boisson-Dupuis S, Thimme R, Weidmann M, Casanova JL, Haller O, Kochs G (2007) Induction of MxA gene expression by influenza A virus requires type I or type III interferon signaling. J Virol 81:7776–7785

Horisberger MA, McMaster GK, Zeller H, Wathelet MG, Dellis J, Content J (1990) Cloning and sequence analyses of cDNAs for interferon- and virus-induced human Mx proteins reveal that they contain putative guanine nucleotide-binding sites: functional study of the corresponding gene promoter. J Virol 64:1171–1181

Kong XF, Zhang XX, Gong QM, Gao J, Zhang SY, Wang L, Xu J, Han Y, Jin GD, Jiang JH, Zhang DH, Lu ZM (2007) MxA induction may predict sustained virologic responses of chronic hepatitis B patients with IFN-alpha treatment. J Interferon Cytokine Res 27:809–818

Leong DT, Gupta A, Bai HF, Wan G, Yoong LF, Too HP, Chew FT, Hutmacher DW (2007) Absolute quantification of gene expression in biomaterials research using real-time PCR. Biomaterials 28:203–210

Mahanonda R, Sa-Ard-Iam N, Rerkyen P, Thitithanyanont A, Subbalekha K, Pichyangkul S (2012) MxA expression induced by alpha-defensin in healthy human periodontal tissue. Eur J Immunol 42:946–956

McGilvray I, Feld JJ, Chen L, Pattullo V, Guindi M, Fischer S, Borozan I, Xie G, Selzner N, Heathcote EJ, Siminovitch K (2012) Hepatic cell-type specific gene expression better predicts HCV treatment outcome than IL28B genotype. Gastroenterology 142:1122–1131

Peng XM, Lei RX, Gu L, Ma HH, Xie QF, Gao ZL (2007) Influences of MxA gene−88 G/T and IFN-gamma +874 A/T on the natural history of hepatitis B virus infection in an endemic area. Int J Immunogenet 34:341–346

Prescott J, Ye C, Sen G, Hjelle B (2005) Induction of innate immune response genes by Sin Nombre hantavirus does not require viral replication. J Virol 79:15007–15015

Randall RE, Goodbourn S (2008) Interferons and viruses: an interplay between induction, signalling, antiviral responses and virus countermeasures. J Gen Virol 89:1–47

Ronni T, Matikainen S, Lehtonen A, Palvimo J, Dellis J, Van Eylen F, Goetschy JF, Horisberger M, Content J, Julkunen I (1998) The proximal interferon-stimulated response elements are essential for interferon responsiveness: a promoter analysis of the antiviral MxA gene. J Interferon Cytokine Res 18:773–781

Sadler AJ, Williams BR (2008) Interferon-inducible antiviral effectors. Nat Rev Immunol 8:559–568

Schimmer BP, White PC (2010) Minireview: steroidogenic factor 1: its roles in differentiation, development, and disease. Mol Endocrinol 24:1322–1337

Torisu H, Kusuhara K, Kira R, Bassuny WM, Sakai Y, Sanefuji M, Takemoto M, Hara T (2004) Functional MxA promoter polymorphism associated with subacute sclerosing panencephalitis. Neurology 62:457–460

Tran Thi Duc T, Desmecht D, Cornet A (2012) Functional characterization of new allelic polymorphisms identified in the promoter region of the human MxA gene. Int J Immunogenet. doi:10.1111/j.1744-313X.2012.01153.x

Inhalation Toxicology

http://informahealthcare.com/iht
ISSN: 0895-8378 (print), 1091-7691 (electronic)

Inhal Toxicol, 2013; 25(5): 298–306
 DOI: 10.3109/08958378.2013.780116

informa healthcare

RESEARCH ARTICLE

Inhalation carcinogenicity of 1,1,1-trichloroethane in rats and mice

Makoto Ohnishi, Yumi Umeda, Taku Katagiri, Tatsuya Kasai, Naoki Ikawa, Tomoshi Nishizawa, and Shoji Fukushima

Japan Bioassay Research Center, Japan Industrial Safety and Health Association, Hadano, Kanagawa, Japan

Abstract

Carcinogenicity of 1,1,1-trichloroethane (TCE) was examined by an inhalation exposure of F344 rats and BDF1 mice of both sexes to TCE at 0, 200, 800 or 3200 ppm for 6 h/d, 5 d/week for 104 weeks. In male rats, the incidences of bronchiolo-alveolar adenomas and peritoneal mesotheliomas were significantly increased in the 800 and 3200 ppm-exposed groups, respectively. The incidence of bronchiolo-alveolar adenomas in the 3200 ppm-exposed groups exceeded the range of historical control data in the Japan Bioassay Research Center. In female rats, the tumor incidences were not increased in any organs of the TCE-exposed groups. In male mice, a significant positive trend with dose was shown for incidences of bronchiolo-alveolar carcinomas, combined incidences of bronchiolo-alveolar adenomas/carcinomas and hepatocellular adenomas. The incidence of Harderian gland adenomas was significantly increased in the 3200 ppm-exposed group, and malignant lymphomas of spleen at this highest dose exceeded the range of historical control data. In female mice, the combined incidence of bronchiolo-alveolar adenomas/carcinomas was significantly increased in the 3200 ppm-exposed group, and the incidences of hepatocellular adenomas and combined incidences of hepatocellular adenomas/carcinomas were significantly increased in the 200, 800 and 3200 ppm-exposed groups with dose dependence except the combined incidence of hepatocellular adenomas/carcinomas in the 200 ppm-exposed group. The incidences of bronchiolo-alveolar adenomas in the 3200 ppm-exposed group and combined incidences of hepatocellular adenomas/carcinomas in the 200 ppm-exposed groups exceeded the ranges of historical control data. Thus, this study provided clear evidence of inhalation carcinogenicity for TCE in both rats and mice.

Keywords

1,1,1-Trichloroethane, carcinogenicity, inhalation, mouse, rat

History

Received 25 January 2013
Revised 15 February 2013
Accepted 22 February 2013
Published online 24 April 2013

Introduction

1,1,1-Trichloroethane (TCE: CAS. 71-55-6) is one of the compounds addressed by the Montreal Protocol, which stipulates that the production and consumption of potentially ozone-depleting substances in the stratosphere are to be phased out. Under the Montreal Protocol, the final phase-out for developed countries for TCE was 1996, with selected exceptions for existing stocks and essential uses; developing countries having until 2015 for their ban to take effect (UNEP, 2003). Subsequently, its atmospheric concentration has declined steadily (Montzka et al., 1996, 1999; Reimann et al., 2005). It was reported that the atmospheric concentration of TCE was 0.025 ppb at Jungfraujoch, Switzerland and at Mach Head, Ireland in 2003 (Reimann et al., 2005). In Japan, the environmental atmospheric concentration of TCE was about 0.02 ppb in Iwate prefecture in 2010 (WMO, 2012).

Address for correspondence: Makoto Ohnishi, PhD, Japan Bioassay Research Center, Japan Industrial Safety and Health Association, 2445 Hirasawa, Hadano, Kanagawa 257-0015, Japan. Tel: +81-463-82-3911. Fax: +81-463-82-3860. E-mail: m-onishi@jisha.or.jp

TCE was tested for carcinogenicity in rats and mice by the inhalation exposure in a previous study (Quast et al., 1988), which found no evidence of any carcinogenic effects in either species. The International Agency for Research on Cancer (IARC) classified TCE as a Group 3 carcinogen (not classifiable as to its carcinogenicity to humans) in 1999 (IARC, 1999). The American Conference of Government Industrial Hygienists (ACGIH) also assessed TCE carcinogenicity as A4 (not classifiable as a human carcinogen) in 1996 (ACGIH, 2001) and the Japan Society for Occupational Health (JSOH, 2010) recommended the occupational exposure limit to be 200 ppm based on the central nervous system depressing effects of TCE. Importantly, in the Integrated Risk Information System (IRIS) report, the exposure levels employed in the carcinogenicity tests were too low (U.S. EPA, 2007). The maximum tolerated dose (MTD) was not reached in mice (no adverse effects observed in either sex) and may not have been reached in rats, as the only toxic effects noted were a slight reduction in body weight gain in female rats and slight microscopic hepatic changes in male and female rats exposed to the high concentration of 1500 ppm. Therefore, the possibility of tumors occurring at higher inhalation exposures cannot be ruled out.

With the purpose of providing hazard data for the carcinogenic risk assessment of TCE, the dose–response

relationship between inhalation exposure concentrations of TCE and inhalation carcinogenicity responses was therefore examined here using F344 rats and BDF1 mice of each sex in a 2-year inhalation study.

Materials and methods

This study was conducted with reference to the Organization for Economic Cooperation and Development (OECD) Guideline for Testing of Chemicals 451 "Carcinogenicity Studies" (OECD, 1981a), and in accordance with the OECD Principles of Good Laboratory Practice (OECD, 1981b). The animals were cared for in accordance with the Guideline for Animal Experimentation (Japanese Association for Laboratory Animal Science, 1987). This study was approved by the ethics committee of the Japan Bioassay Research Center (JBRC).

Chemicals

Analytical-grade TCE (greater than 95% purity, including 1,4-dioxane ranging from 3.34% to 3.50%) was obtained from Wako Pure Chemical Industries, Ltd. (Osaka, Japan). Each lot of the TCE used in this study was analyzed for its purity and stability by gas chromatography and infrared spectrometry before and after its use. Neither decomposition products nor other impurities were detected. No gas chromatographic peak other than TCE was detected in the inhalation exposure chambers.

Animals

F344/DuCrj (SPF) rats and Crj: BDF1 (SPF) mice of both sexes were obtained at 4 weeks of age from Charles River Japan, Inc. (Kanagawa, Japan). The animals were quarantined and acclimated for 2 weeks, and then divided by stratified randomization into four body weight-matched groups, each comprising 50 rats and 50 mice of both sexes. The animals were housed individually in stainless-steel wire hanging cages (125 mm [W] × 216 mm [D] × 176 mm [H] for rats and 95 mm [W] × 116 mm [D] × 120 mm [H] for mice) in stainless steel inhalation exposure chambers from Sibata Scientific Technology Ltd. (Saitama, Japan) maintained at a temperature of 23 °C ± 2 °C and at a relative humidity of 55% ± 10%. The chamber for rats and mice consists of three parts, one rectangular parallelepiped and two quadrangular pyramid. The sizes of rectangular parallelepiped are 3.00 m [W] × 1.80 m [D] × 1.00 m [H] and quadrangular pyramid are 2.16 m [W] × 1.30 m [D] × 1.00 m [H] for rats. The sizes of rectangular parallelepiped are 1.50 m [W] × 1.80 m [D] × 1.24 m [H] and quadrangular pyramid are 1.08 m [W] × 1.30 m [D] × 0.93 m [H] for mice. Fluorescent lighting was controlled automatically to give a 12-h light/dark cycle. All rats and mice had free access to sterilized water and γ-irradiation-sterilized commercial pellet diet (CRF-1, Oriental Yeast Co., Ltd., Tokyo, Japan). The body weights measured immediately before the first exposure to TCE or clean air were 122–144 g for male rats, 95–112 g for female rats, 20.2–25.4 g for male mice and 15.9–20.4 g for female mice.

Experimental design

Groups of 50 male and 50 female rats and mice were exposed to airflow containing TCE vapor at target concentrations of 200, 800 or 3200 ppm (v/v) for 6 h/d, 5 d/week and for 104 weeks. Fifty rats and 50 mice of both sexes, serving as respective controls, were handled in the same manner as the TCE-exposed groups, but exposed to clean air in the inhalation exposure chambers. The highest concentration of 3200 ppm was selected based on body weight decrement and other toxicity data from a 13-week inhalation exposure study conducted at the JBRC. Male rats exhibited decreased body weight during a period of 13-week exposure to 4400 ppm TCE, but 13-week exposure to 3000 ppm TCE did not cause body weight decrement or overt toxicity. Male and female mice died during a 13-week period of exposure to 10 000 ppm, and one out of 10 female mice died during a period of 13-week exposure to 6700 ppm, but 13-week exposure of female mice to 4400 and 3000 ppm TCE did not cause clear body weight decrement or overt toxicity. Therefore, it was decided that the highest exposure concentration in the present carcinogenicity test should be 3200 ppm in rats and mice.

Exposure to TCE

Airflow containing TCE vapor at target concentrations of 200, 800 or 3200 ppm was prepared by a vaporization technique. Saturated vapor–air mixtures were generated by bubbling clean air through TCE liquid in a temperature-regulated glass flask (40 °C), and by cooling through a thermostatted condenser at 18 °C. Airflow containing the saturated vapor was diluted with clean air, and then warmed to 40 °C in a thermostatted circulator which served to stabilize the vapor concentration by complete gasification of TCE. The flow rate of the vapor–air mixtures was regulated with a flow meter, and after further dilution with humidity- and temperature-controlled clean air in a spiraling line mixer, they were supplied to inhalation exposure chambers. Four inhalation exposure chambers of 7600 L in volume for rats and four of 3700 L for mice were used in this study. The air change rate in the exposure chamber was 6 ± 1 air changes/h. Each exposure chamber accommodated 100 individual cages for 50 males and 50 females of either rats or mice. Chamber concentrations of TCE were monitored by gas chromatography for every 15 min, and maintained constant at 200.4 ± 4.1 (mean ± SD), 796.6 ± 8.8 and 3181.1 ± 34.1 ppm for the exposure of rats and at 200.6 ± 3.3, 800.6 ± 8.7 and 3204.3 ± 24.0 ppm for the exposure of mice throughout the 2-year exposure period.

Clinical observations and analysis, and pathological examination

The animals were observed daily for clinical signs and mortality. Body weight and food consumption were measured once a week for the first 14 weeks, and every 4 weeks thereafter. Urinary parameters were measured in the last week of the 2-year exposure period with Ames Reagent Strips (Multistix for rats and Uro-Labstix for mice, Siemens

Healthcare Diagnostics Inc., Tarrytown, NY). Blood was collected for blood biochemistry from abdominal aorta under anesthesia after overnight fasting at the end of the 2-year exposure period. The blood samples were analyzed with an automatic analyzer (Hitachi 705, Hitachi, Ltd., Ibaraki, Japan) and a flame photometer (Hitachi 750, Hitachi, Ltd., Ibaraki, Japan) for blood biochemistry.

All rats and mice underwent complete necropsy, when organs were removed, weighed and examined for macroscopic lesions. All organs and tissues indicated in the OECD test guideline (OECD, 1981a) and the entire respiratory tract, including the nasal cavity, pharynx and larynx, were sampled for histopathology in all the animals. The organs and tissues were fixed in 10% neutral buffered formalin, routinely processed for embedding in paraffin, and 3 μm-thick sections were prepared and stained with hematoxylin and eosin (H & E).

Statistics and data analysis

Incidences of neoplastic lesions were analyzed for any dose–response relationship indicated by a significant positive trend by Peto's test (Peto et al.,1980) and for significant differences from the clean air-exposed group by Fisher's exact test. Incidences of non-neoplastic lesions and urinary parameters were analyzed by Chi-square test. Survival curves were plotted according to the method of Kaplan–Meier (1958), and the log-rank test (Peto et al., 1977) and Fisher's exact test were used to test a statistically significant difference in survival rate between any TCE-exposed rat or mouse group of either sex and the relevant clean air-exposed group. Body weights, organ weights and blood biochemical parameters were analyzed by Dunnett's test. All tests were two-tailed test except for the Peto's test and Fisher's exact test. In all cases, a p value of 0.05 was used as the level of significance.

Results

Rat study

Survival, body weights, food consumption and clinical analyses

There were no significant differences in the survival rates between any of the TCE-exposed groups and the controls in both male and female (Figure 1).

In male rats, the terminal survival rates of 0 (control), 200, 800 and 3200 ppm-exposed groups were 68%, 72%, 72% and 56%. Tumor deaths started to occur at the 72nd week with a peritoneal mesothelioma in the 3200 ppm-exposed group. Microscopic examination of rats dying before the end of the 2-year exposure period revealed that 10 males died of peritoneal mesotheliomas in the 3200 ppm-exposed male group. Therefore, the decreased survival rate in the 3200 ppm-exposed group were attributed to the increased number of neoplasm-related deaths, although statistical significance was not observed. Growth rates of TCE-exposed groups were not significantly decreased as compared with the controls (Figure 2). The terminal body weight of 3200 ppm-exposed male rats was 96% of that of the controls. The body weights of 0, 200, 800 and 3200 ppm-exposed groups at the end of the 2-year exposure period were 429 ± 45, 438 ± 23, 442 ± 36 and 410 ± 33 g.

In female rats, the terminal survival rates of 0 (control), 200, 800 and 3200 ppm-exposed groups were 76%, 76%, 84% and 76%. Growth rates of TCE-exposed groups were not

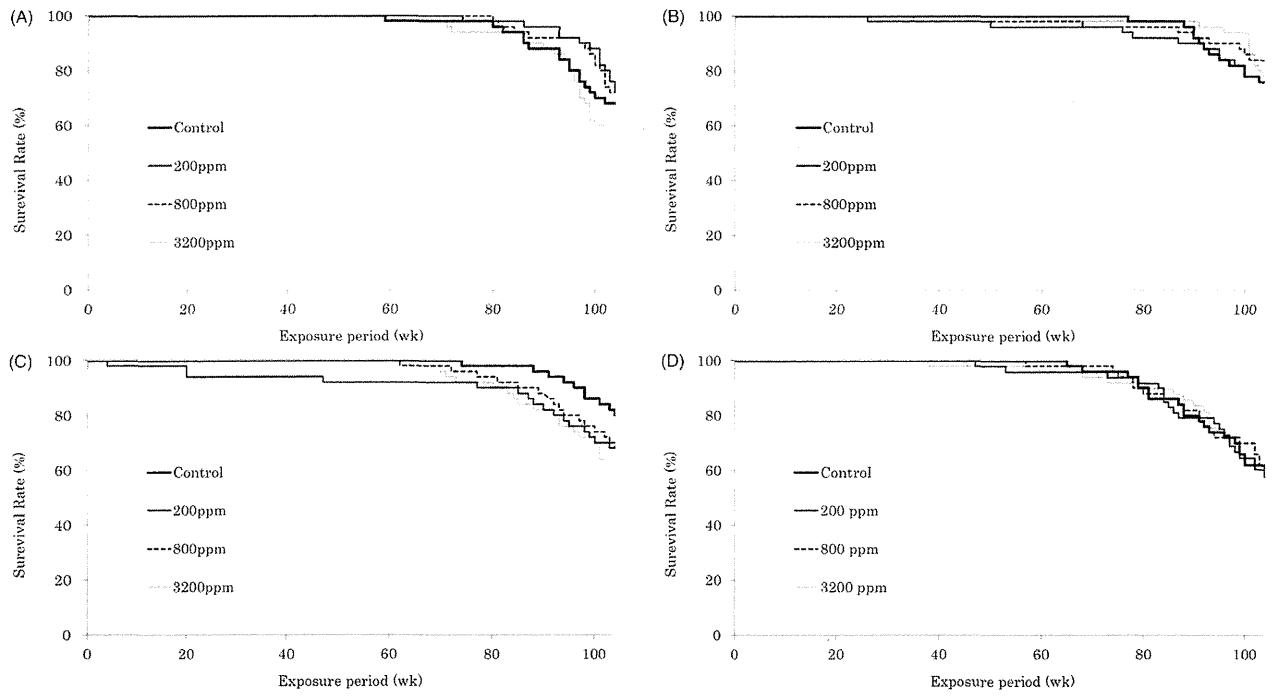

Figure 1. Survival curves of both rats and mice exposed to TCE vapor at 200, 800 and 3200 ppm and clean air as the control for 2-year. (A) Male rats. (B) Female rats. (C) Male mice. (D) Female mice.

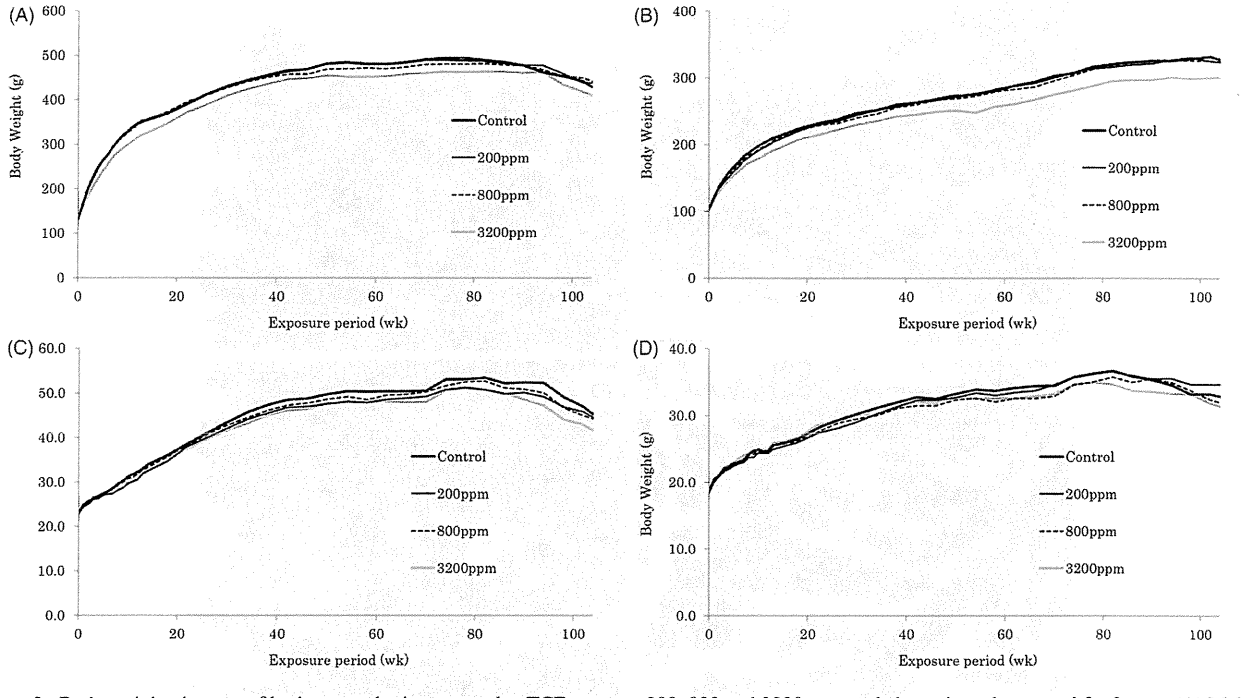

Figure 2. Body weight changes of both rats and mice exposed to TCE vapor at 200, 800 and 3200 ppm and clean air as the control for 2-year. (A) Male rats. (B) Female rats. (C) Male mice. (D) Female mice.

Table 1. Numbers of rats exposed to 1,1,1-trichloroethane by inhalation for 2-year.

Groups	Control	200 ppm	800 ppm	3200 ppm	Peto's	JBRC historical control data	
Number of animals	50	50	50	50	test	Incidence[a]	Min–Max[b]
Male							
Lung							
Bronchiolo-alveolar adenoma	0 (0.0%)	1 (2.0%)	**7** (14.0%)#	**4** (8.0%)	↑	16/649 (2.5%)	0/50-3/50 (0-6%)
Peritoneum							
Mesothelioma	1 (2.0%)	2 (4.0%)	1 (2.0%)	**16** (32.0%)##	↑↑	17/649 (2.6%)	0/50-4/50 (0-8%)
Female							
Lung							
Bronchiolo-alveolar adenoma	1 (2.0%)	1 (2.0%)	2 (4.0%)	0 (0.0%)		13/649 (2.0%)	0/50-3/50 (0-6%)
Peritoneum							
Mesothelioma	1 (2.0%)	0 (0.0%)	0 (0.0%)	0 (0.0%)		1/649 (0.2%)	0/50-1/50 (0-2%)

and ## Significantly different from the control group at $p \leq 0.05$ and $p \leq 0.01$ by Fisher's exact test, respectively.
↑ and ↑↑ Significantly different at $p \leq 0.05$ and $p \leq 0.01$ by Peto's test, respectively.
[a]Number of animals bearing tumor/number of animals examined in the 13 historical inhalation studies.
[b]Number of animals bearing tumor/number of animals examined in a single historical study.
The bold and underlined values indicate the tumor incidences exceeding the maximum tumor incidence in the JBRC historical control data.

significantly decreased as compared with the controls (Figure 2). The terminal body weight of the 3200 ppm-exposed group was 91% of that of the controls. The body weights of 0, 200, 800 and 3200 ppm-exposed groups at the end of 2-year exposure period were 328 ± 28, 324 ± 37, 325 ± 30 and 298 ± 53 g.

In both male and female rats, food consumption was not suppressed in any TCE-exposed groups as compared with the respective controls. No exposure-related changes in any hematological, blood biochemical or urinary parameter were found in any TCE-exposed groups.

Pathology

In female rats, the relative lung, kidney and brain, weights of the 3200 ppm TCE-exposed group were significantly increased as compared with those of the controls, although in male rats, organ weights were not significantly increased.

Macroscopic examination at necropsy revealed that incidences of peritoneal nodules and brown-colored ascites were significantly increased in male rats exposed to 3200 ppm TCE. Table 1 presents incidences of selected tumors in rats exposed by inhalation to TCE or clean air (the controls) for 2-year, with reference to the tumor incidences in the JBRC historical control data.

In male rats, a significant positive trend was shown for incidences of bronchiolo-alveolar adenomas in the lung and mesotheliomas in the peritoneum by Peto's test. The Fisher's exact test demonstrated that the bronchiolo-alveolar adenomas were significantly increased in the 800 ppm-exposed rats and the incidence of bronchiolo-alveolar adenomas in the

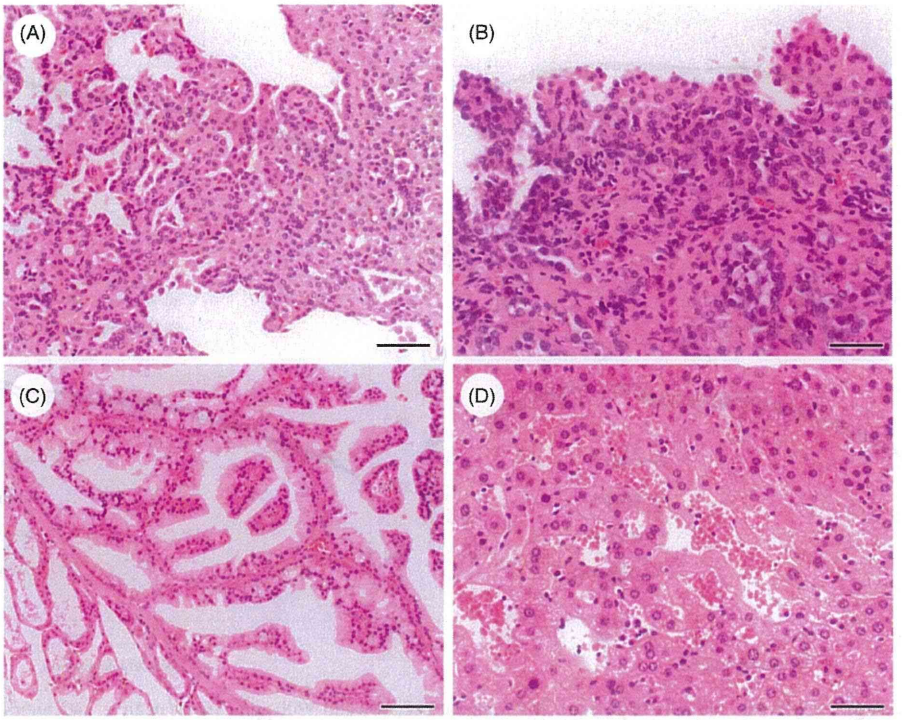

Figure 3. (A) A bronchiolo-alveolar adenoma in the lung of a male rat exposed to 3200 ppm TCE for 2-year. Bar indicates 100 μm. H&E stain. (B) A peritoneal mesothelioma in a male rat exposed to 3200 ppm TCE for 2-year. Bar indicates 50 μm. H&E stain. (C) Harderian gland adenoma of a male mouse exposed to 3200 ppm TCE for 2-year. Bar indicates 100 μm. H&E stain. (D) Hepatocellular adenoma in the liver of a female mouse exposed to 3200 ppm TCE for 2-year. Bar indicates 250 μm. H&E stain.

800 and 3200 ppm-exposed groups exceeded the respective maximum tumor incidences of the historical control data of JBRC, although the incidence in the 3200 ppm-exposed group was less than that in the 800 ppm-exposed rats. Histopathologically, the bronchiolo-alveolar adenomas were distinct masses with glandular patterns of tumor cells (Figure 3A). Those tumors compressed surrounding alveolar spaces. Peritoneal mesotheliomas were significantly increased in the 3200 ppm-exposed male rats, and their incidence exceeded the maximum tumor incidence in the historical control data. The mesotheliomas involved the surface of the peritoneal cavity, especially the scrotal sac, and were composed of one to several layers of the neoplastic mesothelial cells covering pedunculated fibrovascular stalks (Figure 3B). In female rats, incidences of tumors were not increased in the TCE-exposed groups.

Exposure-related, neoplastic lesions other than those described in Table 1 were not observed in either male or female rats. As a non-neoplastic lesion, eosinophilic change of the olfactory epithelium in the nasal cavity and cortical hyperplasia in the adrenals were observed at slightly increased severity (nasal cavity) and incidence (adrenal) in the females exposed to 3200 ppm.

Mouse study

Survival, body weights, food consumption and clinical analyses

The survival rates of the TCE-exposed groups and controls are shown in Figure 1.

In males, slightly decreased survival of the 3200 ppm-exposed group was observed. However, there was no significant difference in the survival rate at any time point of the 2-year exposure period between the 200 and 800 ppm-exposed groups and the controls. The terminal survival rates of 0 (control), 200, 800 and 3200 ppm-exposed groups were 80%, 68%, 68% and 62%. Growth rates of TCE-exposed groups were not significantly decreased as compared with the controls (Figure 2). The body weights of the 0, 200, 800 and 3200 ppm-exposed groups at the end of the 2-year exposure period were 45.2 ± 6.4, 44.6 ± 7.5, 44.3 ± 6.6 and 41.6 ± 6.2 g.

In female mice, there were no significant differences in the survival rates between any TCE-exposed group and the controls. The terminal survival rates of 0 (control), 200, 800 and 3200 ppm-exposed group were 58%, 58%, 58% and 59%. Growth rates of TCE-exposed groups were not significantly decreased as compared with the controls (Figure 2). The body weights of 0, 200, 800 and 3200 ppm-exposed groups at the end of 2-year exposure period were 32.9 ± 4.8, 34.7 ± 3.5, 32.0 ± 4.2 and 31.4 ± 3.2 g.

In male and female mice, food consumption was not suppressed in any TCE-exposed group of either sex as compared with the respective controls. Dose-related changes in hematological or blood chemical parameters measured at the end of the 2-year exposure period were not observed in any TCE-exposed groups (data not shown), although statistical significance was found sporadically for some of those parameters. Urinalysis at the last week of the 2-year exposure period demonstrated increased ketone bodies in the 3200 ppm-exposed male mice.

Table 2. Numbers of tumors in male mice exposed to 1,1,1-trichloroethane by inhalation for 2-year.

Groups	Control	200 ppm	800 ppm	3200 ppm	Peto's	JBRC historical control data	
Number of animals	50	50	50	50	test	Incidence[a]	Min–Max[b]
Lung							
Bronchiolo-alveolar adenoma	4 (8.0%)	8 (16.0%)	4 (8.0%)	1 (2.0%)		46/598 (7.7%)	2/50–9/50 (4.0–18.0%)
Bronchiolo-alveolar carcinoma	3 (6.0%)	5 (10.0%)	6 (12.0%)	10 (20.0%)	↑↑	67/598 (11.2%)	1/50–11/50 (2.0–22.0%)
Combined bronchiolo-alveolar adenoma/carcinoma	7 (14.0%)	13 (26.0%)	10 (20.0%)	11 (22.0%)	↑	113/598 (18.9%)	3/50–14/50 (6.0–28.0%)
Liver							
Hepatocellular adenoma	10 (20.0%)	8 (16.0%)	12 (24.0%)	15 (30.0%)	↑	101/598 (16.9%)	2/50–15/50 (4.0–30.0%)
Hepatocellular carcinoma	14 (28.0%)	12 (24.0%)	10 (20.0%)	15 (30.0%)		148/598 (24.7%)	1/50–18/50 (2.0–36.0%)
Combined hepatocellular adenoma/carcinoma	23 (46.0%)	19 (38.0%)	21 (42.0%)	26 (52.0%)		225/598 (37.6%)	4/50–30/50 (8.0–60.0%)
Spleen							
Malignant lymphoma	3 (6.0%)	4 (8.0%)	3 (6.0%)	**9** (18.0%)	↑↑	24/597 (4.0%)	1/50–4/50 (2.0–8.0%)
Harderian gland							
Adenoma	1 (2.0%)	4 (8.0%)	4 (8.0%)	**8** (16.0%)#	↑↑	30/598 (5.0%)	1/50–5/50 (2.0–10.0%)

Significantly different from the control group at $p \leq 0.05$ by Fisher's exact test, respectively.
↑ and ↑↑ Significantly different at $p \leq 0.05$ and $p \leq 0.01$ by Peto's test, respectively.
[a]Number of animals bearing tumor/number of animals examined in the 12 historical inhalation studies.
[b]Number of animals bearing tumor/number of animals examined in a single historical study.
The bold and underlined values indicate the tumor incidences exceeding the maximum tumor incidence in the JBRC historical control data.

Table 3. Numbers of tumors in female mice exposed to 1,1,1-trichloroethane by inhalation for 2-year.

Groups	Control	200 ppm	800 ppm	3200 ppm	Peto's	JBRC historical control data	
Number of animals	50	48	50	49	test	Incidence[a]	Min–Max[b]
Lung							
Bronchiolo-alveolar adenoma	0 (0.0%)	0 (0.0%)	0 (0.0%)	**5** (10.2%)	↑↑	23/599 (3.8%)	0/50–5/50 (0.0–10.0%)
Bronchiolo-alveolar carcinoma	1 (2.0%)	**3** (6.3%)	1 (2.0%)	2 (4.1%)		17/599 (2.8%)	0/50–3/50 (0.0–6.0%)
Combined bronchiolo-alveolar adenoma/carcinoma	1 (2.0%)	3 (6.3%)	1 (2.0%)	**7** (14.3%)#	↑↑	40/599 (6.7%)	1/50–6/50 (2.0–12.0%)
Liver							
Hepatocellular adenoma	2 (4.0%)	**9** (18.8%)#	**14** (28.0%)##	**19** (38.8%)##	↑↑	29/599 (4.8%)	1/50–5/50 (2.0–10.0%)
Hepatocellular carcinoma	2 (4.0%)	1 (2.1%)	2 (4.0%)	1 (2.0%)		12/599 (2.0%)	0/50–2/50 (0.0–4.0%)
Combined hepatocellular adenoma/carcinoma	4 (8.0%)	**10** (20.8%)	**16** (32.0%)#	**20** (40.8%)##	↑↑	40/599 (6.7%)	1/50–6/50 (2.0–12.0%)
Spleen							
Malignant lymphoma	4 (8.0%)	4 (8.3%)	5 (10.0%)	3 (6.1%)		33/599 (5.5%)	1/50–7/50 (0.0–14.0%)
Harderian gland							
Adenoma	3 (6.0%)	4 (8.3%)	1 (2.0%)	2 (4.1%)		20/599 (3.3%)	1/50–6/50 (0.0–12.0%)

and ## Significantly different from the control group at $p \leq 0.05$ and $p \leq 0.01$ by Fisher's exact test, respectively.
↑ and ↑↑ Significantly different at $p \leq 0.05$ and $p \leq 0.01$ by Peto's test, respectively.
[a]Number of animals bearing tumor/number of animals examined in the 12 historical inhalation studies.
[b]Number of animals bearing tumor/number of animals examined in a single historical study.
The bold and underlined values indicate the tumor incidences exceeding the maximum tumor incidence in the JBRC historical control data.

Pathology

There were no significant differences in weights of various organs between any TCE-exposed groups and the respective male and female controls.

Macroscopic examination at necropsy revealed that the incidences of nodules in the liver were increased in an exposure concentration-related manner in female mice. These nodules in the liver were histopathologically diagnosed as hepatocellular adenomas or carcinomas. Tables 2 and 3 present selected tumor incidences in mice of both sexes exposed to TCE or clean (the control) air for 2-year, with reference to the tumor incidences of the JBRC historical control data.

In male mice, a significant positive trend was shown for the incidences of bronchiolo-alveolar carcinomas and combined incidences of bronchiolo-alveolar adenomas and carcinomas (adenomas/carcinomas) in the lung, hepatocellular adenomas, malignant lymphoma of spleen and Harderian gland adenoma by Peto's test. Malignant lymphomas of spleen were not significantly increased in any of the TCE-exposed groups, although the incidence in the 3200 ppm-exposed group exceeded the maximum tumor incidence in the historical control data. Harderian gland adenomas, composed of cuboidal to tall columnar cells with papillary growth and abundant, foamy, pale cytoplasm (Figure 3C), were significantly increased in the 3200 ppm-exposed mice by Fisher's exact test and the incidence exceeded the maximum tumor incidence in the historical control data. Exposure-related neoplastic lesions other than those listed in Table 2 were not observed.

In female mice, a significant positive trend was shown for incidences of bronchiolo-alveolar adenomas, and combined

incidences of bronchiolo-alveolar adenomas/carcinomas in the lung by Peto's test. In the same test, significant positive trends were shown for hepatocellular adenomas and combined incidences of hepatocelluar adenomas/carcinomas. The incidence of bronchiolo-alveolar adenomas in the 3200 ppm-exposed group exceeded the maximum tumor incidence in the historical control data. In addition, the combined incidence of bronchiolo-alveolar adenomas/carcinomas was significantly increased in the 3200 ppm-exposed group by Fisher's exact test, and the incidence exceeded the respective maximum tumor incidence in the historical control data. Hepatocellular adenomas were significantly increased in the 200, 800 and 3200 ppm-exposed groups by Fisher's exact test, and the incidences exceeded the respective maximum tumor incidence in the historical control data. The combined incidence of hepatocellular adenomas/carcinomas significantly increased in the 800 and 3200 ppm-exposed mice, and the tumor incidences in the 200, 800 and 3200 ppm-exposed groups exceeded the respective maximum tumor incidences of the historical control data. The hepatocellular adenomas were well-circumscribed lesions compressing adjacent parenchyma and lacking normal lobular architecture, composed of well-differentiated hepatocytes (Figure 3D). Exposure-related, neoplastic lesions other than those listed in Table 3 were not observed in female mice. No exposure-related non-neoplastic lesions occurred in any of the TCE-exposed groups.

Discussion

This study demonstrated that 2-year inhalation exposure to TCE vapor significantly increased incidences of benign and malignant tumors in several organs of rats and mice.

In male rats, bronchiolo-alveolar adenomas in the lung and abdominal peritoneal mesotheliomas were induced by the 2-year exposure to TCE on the basis of the following evidence. Incidences of these tumors were increased in a concentration-dependent manner, with a significant positive trend. The increase in bronchiolo-alveolar adenomas at the 800 ppm group and peritoneal mesotheliomas at the 3200 ppm group attained statistical significance by Fisher's exact test. Additionally, the incidences of those tumors in the 3200 ppm-exposed group, as well as the incidence of bronchiolo-alveolar adenomas in the 800 ppm-exposed group, exceeded the respective maximum tumor incidences in the JBRC historical control data.

In male mice, concentration-dependent increase in the incidences of malignant lymphomas of spleen and Harderian gland adenomas were evidenced by significant positive trends. The increase in Harderian gland tumors in the 3200 ppm group attained statistical significance by Fisher's exact test. In addition, the incidences of tumors (spleen and Harderian gland) in the 3200 ppm-exposed group exceeded the maximum tumor incidence in the historical control data.

In female mice, concentration-dependent increase in the incidences of bronchiolo-alveolar adenomas, bronchiolo-alveolar adenomas/carcinomas combined, hepatocellular adenomas and hepatocellular adenomas/carcinomas combined were evidenced by significant positive trends. The incidences of pulmonary tumors in the 3200 ppm-exposed group exceeded the maximum tumor incidence in the historical control data. The increases of combined incidence of hepatocellurar adenomas/carcinomas in the 800 and 3200 ppm-exposed groups attained statistical significance by Fisher's exact test. Furthermore, the incidences of hepatic tumors in the 200, 800 and 3200 ppm-exposed groups exceeded the maximum incidence in the historical control data.

In the study of Quast et al. (1988), male and female of Fischer 344 rats and B6C3Fl mice were exposed to 0, 150, 500 or 1500 ppm TCE vapor for 6 h/d, 5 d/week for 2 years. Inhalation exposure of Fischer 344 rats to 1500 ppm TCE vapor resulted in a slight reduction of the body weights in females. While very slight microscopic hepatic effects were seen in the livers of 1500 ppm-exposed male and female rats necropsied at 6, 12 and 18 months (using 10 rats), hepatic tumors were not observed at 24 months (using 50 rats). There were no toxic effects noted in mice at any exposure concentrations of TCE. Particularly, there were no indications of oncogenic effects in rats or mice following the 2-year exposure of TCE. However, it was noted in the IRIS report (U.S. EPA, 2007) that the exposure levels were too low, because the MTD was not reached in mice (no adverse effects observed in either sex) and may not have been reached in rats.

In the present carcinogenicity study of rats and mice, selection of the highest concentration, 3200 ppm was appropriate for evaluating carcinogenic potency of TCE for the following reasons. First, terminal body weights of TCE-exposed rats and mice were less than 10% as compared with those of respective controls. Second, there was no significant difference in the survival rate between any of the TCE-exposed rat and mouse groups and the respective controls except for the survival rate of 3200 ppm-exposed male mice. The present data for both 2-year survival rates and the terminal body weight decrease without any overt manifestation of chronic non-neoplastic lesions in the TCE-exposed animals can be taken to fulfill the MTD criteria, indicating that the highest concentrations of 3200 ppm did not exceed the MTD in accordance with the prediction from the 13-week inhalation exposure study.

In this study, the tumors which significantly increased in the female mice exposed to 200 and 800 ppm TCE were hepatocellurar adenomas. Quast et al. (1988) reported that mice exposed to TCE at the highest dose of 1500 ppm did not have tumors in the 2-year study. This study used the Crj: BDF1 mice, whereas Quast used the B6C3F1 mice. Therefore, strain differences may contribute to sensitivity of TCE hepatocarcinogenicity.

The results of mutagenicity studies for TCE with *Salmonella typhimurium* TA100 and TA1535 in the presence and absence of metabolic activation were positive with vapor phase (JETOC, 2005a). The results of chromosome aberrations in cultured Chinese hamster ovary cells were also positive (Galloway et al., 1987). In addition, the results of cell transformation assays were positive (Hatch et al., 1983). Therefore, it is possible that a genotoxic mode of action operates in TCE -induced carcinogenesis.

For the metabolism of TCE, Schumann et al. (1982) reported studies on the pharmacokinetics of [^{14}C] TCE in male Fischer 344 rats and B6C3F1 mice undertaken to

characterize the disposition of the inhaled chemical over a wide range of exposure concentrations. The major elimination route of TCE was via exhalation of unchanged chemical in expired air, accounting approximately 94%–98% of the total recovered radioactivity in rats and 87%–97% in mice at 150 and 1500 ppm, respectively. In addition, Nolan et al. (1984) reported that over 91% of the absorbed TCE was excreted unchanged.

Mesotheliomas are tumors that arise from the serosal surface of the pleura, peritoneum and pericardium. They also originate from the oil-rich tunica vaginalis of the testis manifested as a paratesticular mass (Brimo et al., 2010). The octanol–water partition coefficient (TCE: 2.49) of TCE is higher than the octanol–water partition coefficient (1,2-dichloroethane (DCE): 1.48, dichloromethane (DCM): 1.3) (WHO, 2003a,b,c). Hence, it would be expected that the high lipid soluble TCE was concentrated on the serosal surface of the peritoneum, where it induced mesotheliomas.

The highly significant incidences of peritoneal methotheliomas in male rats and hepatocellular adenomas in the female mice clearly indicate that they were caused by TCE-inhalation exposure. Of note, the incidences of these neoplastic lesions are higher than those in the carcinogenicity study in the rats and mice for inhalation exposure of TCE-related compounds, DCE (Nagano et al., 2006) and DCM (Aiso et al., 2001), carried out by JBRC. Moreover, hepatocellular adenomas were also induced by the administration of DCE and DCM in the female mice, and the sex dependence may be related to the fact that sex differences exist in the reported evidence of DNA adducts and mutagenesis (JETOC, 2005a,b,c). In addition, NTP reported that oral administration of 1,2,3-trichloropropane, a related substance of TCE, resulted in the development of neoplasms of the liver and Harderian gland in male and female mice (NTP, 1993).

In conclusion, the present study provided clear evidence of carcinogenicity for TCE on inhalation exposure in rats and mice.

Acknowledgements

The author thank Ms. Haruka Tomono (Sophia University) for detailed review of this manuscript. We also acknowledge the technical support of Mr Masahiro Yamamoto, Mr Yasutomo Sasaki and Mrs. Mieko Saito.

Declaration of interest

The present studies were contracted and supported by the Ministry of Health, Labour and Welfare of Japan. The authors declare that there are no conflicts of interest.

References

Aiso S, Saito A, Ohsawa M, et al. (2001). Carcinogenesis studies of dichloromethane in F344 rats and BDF1 mice (inhalation study). Proceeding of The Japanese Cancer Association, 60th Annual Meeting. Jpn J Cancer Res 92:277.

American Conference on Governmental Industrial Hygienists (ACGIH). (2001). 1,1,1-Trichloroethane. Documentation of the threshold limit values (TLVs) and biological exposure indices (BEIs) [CD-ROM]. Cincinnati, OH: ACGIH.

Brimo F, Illei PB, Epstein JI. (2010). Mesothelioma of the tunica vaginalis: a series of eight cases with uncertain malignant potential. Mod Pathol 23:1165–72.

Galloway SM, Armstrong MJ, Reuben C, et al. (1987). Chromosome aberrations and sister chromatid exchanges in Chinese hamster ovary cells: evaluations of 108 chemicals. Environ Mol Mutagen 10:1–175.

Hatch GG, Mamay PD, Ayer ML, et al. (1983). Chemical enhancement of viral transformation in Syrian hamster embryo cells by gaseous and volatile chlorinated methanes and ethanes. Cancer Res 43: 1945–50.

International Agency for Research on Cancer (IARC). (1999). 1,1,1-Trichloroethane. Re-evaluation of some organic chemicals, hydrazine and hydrogen peroxide (Part Two). IARC Monogr Eval Carcinogen Risk Hum 71:881–903.

Japan Chemical Industry Ecology-Toxicology & Information Center (JETOC). (2005a). Mutagenicity in bacterial test data of existing chemical substances: based on toxicity investigation system of the Industrial Safety and Health Law (1,1,1-trichloroethane). Tokyo: JETOC, B0105.

Japan Chemical Industry Ecology-Toxicology & Information Center (JETOC). (2005b). Mutagenicity in bacterial test data of existing chemical substances: based on toxicity investigation system of the Industrial Safety and Health Law (1,2-dichloroethane). Tokyo: JETOC, B0009.

Japan Chemical Industry Ecology-Toxicology & Information Center (JETOC). (2005c). Mutagenicity in bacterial test data of existing chemical substances: based on toxicity investigation system of the Industrial Safety and Health Law (dichloromethane). Tokyo: JETOC, B9414.

Japan Society for Occupational Health (JSOH). (2010). Recommendation of occupational exposure limits 1974. J Occup Health 52:313.

Japanese Association for Laboratory Animal Science (JALAS). (1987). Guideline for animal experimentation. Exp Anim 36:285–8.

Kaplan EL, Meier P. (1958). Nonparametric estimation from incomplete observations. Am Stat Assoc J 53:457–81.

Montzka SA, Butler JH, Elkins JW, et al. (1999). Present and future trends in the atmospheric burden of ozone-depleting halogens. Nature 398:690–4.

Montzka SA, Butler JH, Myers RC, et al. (1996). Decline in the tropospheric abundance of halogen from halocarbons: implications for stratospheric ozone depletion. Science 272:1318–22.

Nagano K, Umeda Y, Senoh H, et al. (2006). Carcinogenicity and chronic toxicity in rats and mice exposed by inhalation to 1,2-dichloroethane for two years. J Occup Health 48:424–36.

National Toxicology Program (NTP). (1993). Toxicology and carcinogenesis studies of 1,2,3,-trichloropropane in F344/N rats and B6C3F1 mice (gavage studies). NTP Technical Report Series No. 384. Bethesda: NTP.

Nolan RJ, Freshour NL, Rick DL, et al. (1984). Kinetics and metabolism of inhaled methyl chloroform (1,1,1-trichloroethane) in male volunteers. Fundam Appl Toxicol 4:654–62.

Organization for Economic Cooperation and Development. (1981a). OECD guideline for testing of chemicals 453 ''combined chronic toxicity/carcinogenicity studies''. Adopted May 1981. Paris: OECD.

Organization for Economic Cooperation and Development. (1981b). OECD principles of good laboratory practice. Adopted 1981. Paris: OECD.

Peto R, Pike MC, Armitage P, et al. (1977). Design and analysis of randomized clinical trials requiring prolonged observation of each patient. II. Analysis and examples. Br J Cancer 35:1–39.

Peto R, Pike MC, Day NE, et al. (1980). Guidelines for simple, sensitive significance tests for carcinogenic effects in long-term animal experiments. IARC Monogr Eval Carcinog Risk Chem Hum Suppl 2:311–426.

Quast JF, Calhoun LL, Frauson LE. (1988). 1,1,1-Trichloroethane formulation: a chronic inhalation toxicity and oncogenicity study in Fischer 344 rats and B6C3F1 mice. Fundam Appl Toxicol 11: 611–25.

Reimann S, Manning AJ, Simmonds PG, et al. (2005). Low European methyl chloroform emissions inferred from long-term atmospheric measurements. Nature 433:506–8.

Schumann AM, Fox TR, Watanabe PG. (1982). [^{14}C]Methyl chloroform (1,1,1-trichloroethane): pharmacokinetics in rats and mice following inhalation exposure. Toxicol Appl Pharmacol 62:390–401.

United Nations Environment Programme (UNEP). (2003). The 1987 Montreal Protocol on Substances that Deplete the Ozone Layer as adjusted and amended by the second, fourth and seventh meetings

of the parties. In: Handbook for the International Treaties for the Protection of the Ozone Layer. 4th ed. Nairobi, Kenya: UNEP, 18–39.

U.S. Environmental Protection Agency (EPA). (2007). 1,1,1-Trichloroethane. Integrated Risk Information System (IRIS). EPA. Available from: http://www.epa.gov/iris/toxreviews/0197tr.pdf [last accessed 21 Sept 2012].

WHO. (2003a). 1,1,1-Trichloroethane in drinking-water. Background document for development of WHO Guidelines for Drinking-water Quality. WHO/SDE/WSH/03.04.65 [Online]. Available from: http://www.who.int/water_sanitation_health/dwq/chemicals/111-Trichloroethane.pdf [last accessed 21 Sept 2012].

WHO. (2003b). 1,2-Dichloromethane in drinking-water. Background document for development of WHO guidelines for drinking-water quality. WHO/SDE/WSH/03.04.67 [Online]. Available from: http://www.who.int/water_sanitation_health/dwq/chemicals/12-Dichloroethane.pdf [last accessed 21 Sept 2012].

WHO. (2003c). Dichloroethane in drinking-water. Background document for development of WHO guidelines for drinking-water quality. World Health Organization [Online]. Available from: http://www.who.int/water_sanitation_health/dwq/chemicals/dichloromethane.pdf [last accessed 21 Sept 2012].

World Meterological Organization (WMO). (2012). WMO WDCGG data summary. Japan Meteorological Agency, World Meteorological Organization [Online]. Available from: http://ds.data.jma.go.jp/gmd/wdcgg/products/summary/sum36/sum36.pdf [last accessed 21 Sept 2012].

Ohnishi *et al. Journal of Occupational Medicine and Toxicology* 2013, **8**:30
http://www.occup-med.com/content/8/1/30

JOURNAL OF OCCUPATIONAL MEDICINE AND TOXICOLOGY

METHODOLOGY **Open Access**

Novel method using hybrid markers: development of an approach for pulmonary measurement of multi-walled carbon nanotubes

Makoto Ohnishi[1*], Hirofumi Yajima[2], Tatsuya Kasai[1], Yumi Umeda[1], Masahiro Yamamoto[1], Seigo Yamamoto[3], Hirokazu Okuda[1], Masaaki Suzuki[1], Tomoshi Nishizawa[1] and Shoji Fukushima[1]

Abstracts

Background: Multi-walled carbon nanotubes (MWCNT)s are suspected to induce pulmonary and pleural cancers due to their asbestos-like configurations. Therefore, accurate measurement of inhaled nanotubes in target organs is crucial for assessing cancer risk. Conventionally, nanotubes are measured after combustion at high temperature for conversion into CO_2; however, the sensitivity is poor and the method lacks versatility. We have therefore developed a novel approach using hybrid markers for nanotube analysis, featuring high sensitivity and the capacity to conduct repeated analyses. The method involves adsorption of markers to nanotubes, followed by their desorption and assessment by means of high performance liquid chromatography (HPLC).

Methods: Recovery of MWCNT from rat lungs was conducted, and pulmonary MWCNT amounts were determined using rats intratracheally-exposed to MWCNT aerosol at 5 mg/m^3 for 6 hours/day.

Results: The correlation coefficient for the calibration curve of MWCNT weight and the HPLC area was 0.9991. Consequently, the lower quantitation limit yielded was 0.2 μg. The recovery was 92-98% at approximately 0.4-2.0 μg demonstrating that MWCNTs in the lung could be measured accurately and precisely.

Conclusions: We have developed a novel method using a hybrid marker approach for nanotube analysis, featuring very high sensitivity and the capacity to conduct repeated analyses. We further confirmed correlations between the amounts of nanotubes and markers and pulmonary nanotube measurement demonstrated that trace amounts could be detected with values closely relating to the administered dose, verifying that the method is sensitive and precise.

Keywords: Multi-walled carbon nanotubes, Novel method using hybrid markers, Fine determination, Rat lungs

Background

Carbon nanotubes were discovered by Iijima in 1991 [1] and are generally expected to greatly contribute to society because of their structure, size, mass, characteristics as semiconductors, and other electrical properties. However, multi-walled carbon nanotubes (MWCNT)s, due to their fiber-like structure [2], are suspected of causing toxicity resembling that observed with asbestos. In animal experiments, development of mesothelioma of the peritoneum has been reported in mice and rats administered MWCNT intraperitoneally [3,4], and clearly care needs to be taken to avoid adverse human exposure. In addition, CNTs was found to exacerbate murine allergic airway inflammation via enhanced activation of T helper cell immunity and increased oxidative stress [5].

Therefore, accurate measurement of inhaled nanotubes in target organs is crucial for assessing cancer risk. Also, there is a need to investigate possible accumulation of MWCNT in the lungs after entry through the nasal cavity, the anticipated exposure route in human cases [6-8]. The characteristics of MWCNT include insolubility, a fiber-like structure of carbon chains, and indistinctive optical signals (excluding specialized regions). For this reason, quantitative evaluation of MWCNT cannot be performed

* Correspondence: m-onishi@jisha.or.jp
[1]Japan Bioassay Research Center, Japan Industrial Safety and Health Association, 2445 Hirasawa, Hadano, Kanagawa 257-0015, Japan
Full list of author information is available at the end of the article

by the application of general analytical methods [9-11]. Rather reliance has been placed on weighing and carbon analysis, which do not necessarily provide high sensitivity. Conventionally, nanotubes are measured after combustion at high temperature for conversion into CO_2; however, the sensitivity is poor and the method lacks versatility [12].

Novel methods using hybrid markers are emerging tools for determinations without the need for weight measurement or carbon analysis. Use of a polycyclic aromatic hydrocarbon (PAH) as a marker was reported by Nakashima et al. [13] with adsorption onto MWCNT resulting in a fluorescence quenching effect from the optical perspective [14]; however, investigations have not been conducted on quantitative evaluation of MWCNT by means of adsorbing PAH as a marker, then desorbing and measuring the amount of marker. We have selected benzo[*ghi*]perylene (B(ghi)P) as a marker, for adsorption onto dispersed MWCNT, then desorption using an organic solvent and quantification by HPLC with fluorescence spectroscopy [15,16]. We here document our novel method using the hybrid marker with evidence of its applicability for measurement of MWCNT in the lungs, including after a single exposure in rats.

Methods

Test substance

A MWCNT sample was purchased from Hodogaya Chemical, Co. Ltd. (MWNT-7, Lot No. 080126, Tokyo, Japan) and used in the present study as produced; i.e., without being purified or further sieved. Since MWCNTs are not water soluble, the test substance was suspended in 9.6% phosphate-buffered saline containing 0.1% Tween 80 (TW-mixture) as a colloidal dispersant and subjected to ultrasonication for 20 min with an ultrasonic homogenizer (VP-30S, 20 kHz, 300 W, TAITEC Co., Ltd, Tokyo, Japan).

Animal

Male F344/DuCrlCrlj rats were purchased from Charles River Japan, Inc. (Kanagawa, Japan) at the age of 4 weeks for inhalation exposure and employed at the age of 11 weeks for intratracheal administration and recovery testing. The animals were quarantined and acclimated for 2 weeks, then housed individually in stainless steel wire-mesh hanging cages (170W × 294D × 176H mm) under controlled environmental conditions. For inhalation chambers, the room temperature and the relative humidity were controlled at 23°C ± 2°C and 55% ± 10% with 12 air changes/hour. For intratracheal administration, the room temperature and the relative humidity were controlled at 24°C ± 2°C and 55% ± 10% with 15 to 17 air changes/hour. Fluorescent lighting was controlled automatically to provide a 12-hour light/dark cycle. All rats had free access to sterilized water and γ-irradiation-sterilized commercial pellet diet (CRF-1, Oriental Yeast Co., Ltd., Tokyo, Japan). The animals were cared for in accordance with the Guide for the Care and Use of Laboratory Animals [17], and the present study was approved by the ethics committee of the Japan Bioassay Research Center (JBRC).

Recovery test design

To validate the proposed method, a recovery test was performed by spiking lung tissue. A total of 5 rats were employed, and their lungs were removed for the recovery test. The mean and standard deviation (SD) of body weights were 253.1 ± 12.4 g at the commencement. After inhalational anesthetization with isoflurane gas (Forane, Abbott Japan Co., Ltd., Tokyo, Japan), all rats underwent complete necropsy, when lungs were removed and weighed. The lungs were fixed in 10% neutral buffered formalin at 1 week. Then, a TW-mixture solution containing 2 μg of MWCNT was added and the lungs were measured for MWCNTs as detailed below.

Intratracheal administration test design

A total of 5 rats were used for the intratracheal administration of MWCNT. The initial body weight mean and SD were 262.2 ± 11.7 g. Before intratracheal administration, the ultrasonicated suspension of MWCNTs was further subjected to additional ultrasonication for 30s with a sonicator (US-2, AS ONE Co., Ltd., Tokyo, Japan). After inhalational anesthetization with isoflurane gas (Forane, Abbott Japan Co., Ltd., Tokyo, Japan), the suspension of MWCNT in TW-mixture (0.3 ml) was intratracheally administrated [18], using a microspray cannula of an Intratracheal Aerosolizer (1A-1B, PennCentury, Inc., USA). Rats received MWCNTs at a dose of 2 μg/animal. At subsequent complete necropsy, the lungs and trachea were removed, weighed, and fixed in 10% neutral buffered formalin for 1 week. Then the lungs were assessed for MWCNTs by the method detailed below.

Inhalation exposure test design

Aerosol generation and whole body inhalation exposure to MWCNTs: The system and method for generation of MWCNT aerosols and inhalation exposure of rats to a dry aerosol in chambers were described in detail earlier [19]. Twenty five rats were exposed to MWCNT aerosol at a target concentration of 5 mg/m^3 for 6 hours/day. The mean and SD of body weights were 123.3 ± 6.1 g for all rats. At the end of the six-hour exposure period, anesthetization with isoflurane gas was performed for 5 rats for necropsy, and their left lungs were removed, weighed, fixed in 10% neutral buffered formalin for 1 week and employed for measurement of MWCNT as detailed below. Groups of five remaining animals were necropsied on 1, 7, 28 or 56 days after the exposure for determination of time change in MWCNT deposits.

Sample preparation for generation of a calibration curve

A 10 mg sample of MWCNT was added to 40 ml of TW-mixture and then sonicated during a 30-min cooling period. The solution was diluted to 2 μg/ml with C99, then 0.4, 0.8, 1.2, 1.6 μg/ml C99 additional solutions were prepared as further standards, 0.1 ml of each being used for analysis. The standard solutions were centrifuged (12000 rpm, 10 min), and the supernatants were removed and after addition of 0.5 ml of TW-mixture were stirred and centrifuged.

Acidic preparation

Following removal of the supernatants and addition of 100 μl concentrated sulfuric acid, the resultant solution was stirred and MWCNTs adhering to Nuclepore membrane filters (Whatman; 111109, pore size; 0.8 μm, diameter; 47 mm) were extracted under ultrasound with 1 ml of TW-mixture and 0.5 ml aliquots of MWCNT solution were transferred to glass tubes for HPLC autosample analysis.

Lung digestion

After fixation in 10% neutral buffered formalin for 1 week, lung samples (Figure 1a) were allowed to react with C99 at room temperature overnight [20] (Figure 1b). The digested solution (Figure 1c) was then centrifuged at 12,000 rpm for 10 minutes (Figure 1d) and the supernatant was removed (Figure 1e). A 0.5 ml aliquot of TW-mixture was added followed by stirring and further centrifugation and then "acidic preparation" and "novel

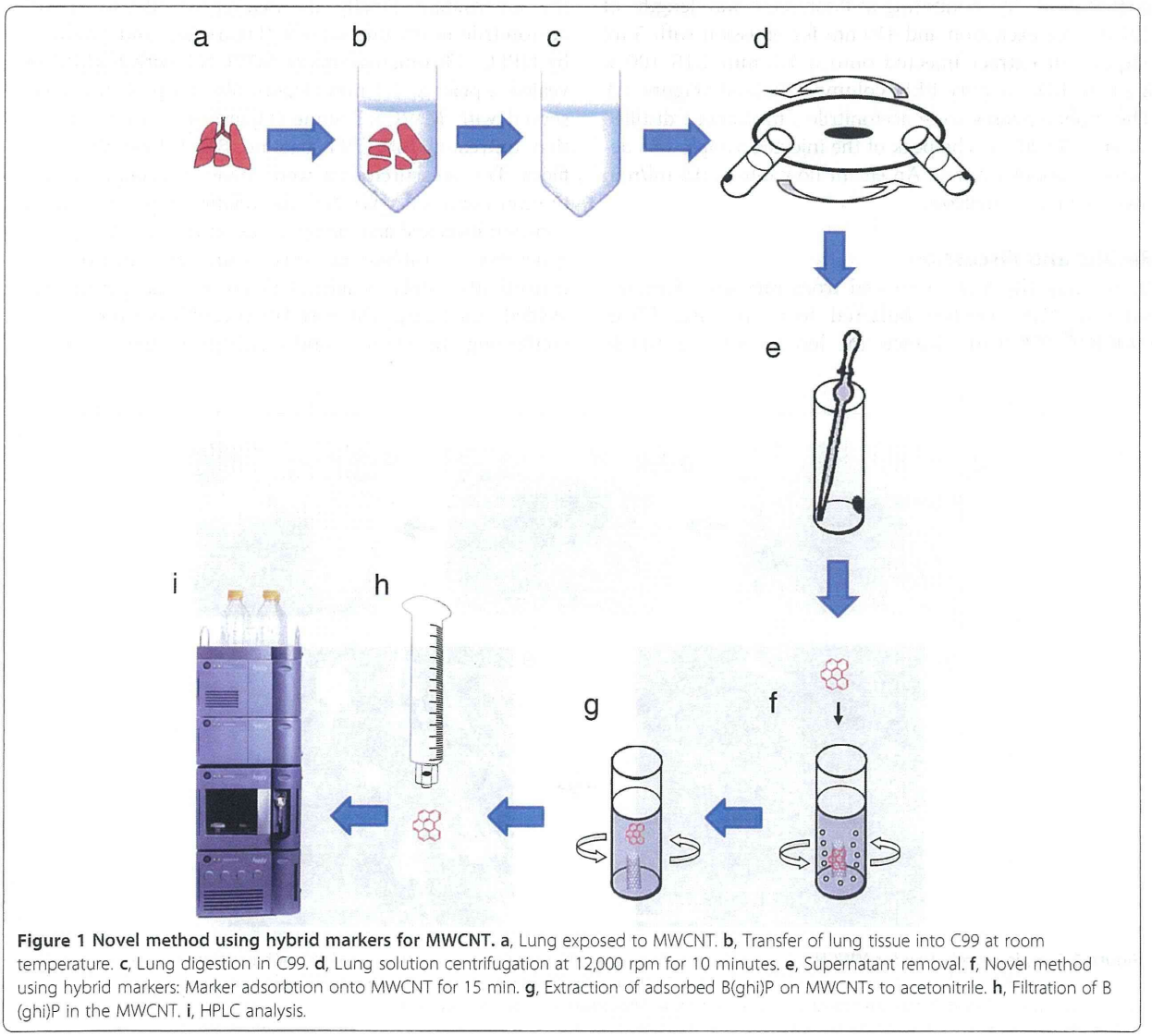

Figure 1 Novel method using hybrid markers for MWCNT. a, Lung exposed to MWCNT. **b**, Transfer of lung tissue into C99 at room temperature. **c**, Lung digestion in C99. **d**, Lung solution centrifugation at 12,000 rpm for 10 minutes. **e**, Supernatant removal. **f**, Novel method using hybrid markers: Marker adsorbtion onto MWCNT for 15 min. **g**, Extraction of adsorbed B(ghi)P on MWCNTs to acetonitrile. **h**, Filtration of B(ghi)P in the MWCNT. **i**, HPLC analysis.